

การสังเคราะห์ไฮโดรคาร์บอนจากเมทานอลบนตัวเร่งปฏิกิริยาฐานโคบอลต์

นางสาวเล อี งาม เอียน



จุฬาลงกรณ์มหาวิทยาลัย  
CHULALONGKORN UNIVERSITY

บทคัดย่อและแฟ้มข้อมูลฉบับเต็มของวิทยานิพนธ์ตั้งแต่ปีการศึกษา 2554 ที่ให้บริการในคลังปัญญาจุฬาฯ (CUIR)

เป็นแฟ้มข้อมูลของนิสิตเจ้าของวิทยานิพนธ์ ที่ส่งผ่านทางบัณฑิตวิทยาลัย

The abstract and full text of theses from the academic year 2011 in Chulalongkorn University Intellectual Repository (CUIR)

วิทยานิพนธ์นี้เป็นส่วนหนึ่งของการศึกษาตามหลักสูตรปริญญาวิทยาศาสตรมหาบัณฑิต

สาขาวิชาเคมีเทคนิค ภาควิชาเคมีเทคนิค  
คณะวิทยาศาสตร์ จุฬาลงกรณ์มหาวิทยาลัย

ปีการศึกษา 2558

ลิขสิทธิ์ของจุฬาลงกรณ์มหาวิทยาลัย

SYNTHESIS OF HYDROCARBONS FROM METHANOL OVER COBALT-BASED CATALYSTS

Miss Le Thi Ngoc Huyen



A Thesis Submitted in Partial Fulfillment of the Requirements  
for the Degree of Master of Science Program in Chemical Technology

Department of Chemical Technology

Faculty of Science

Chulalongkorn University

Academic Year 2015

Copyright of Chulalongkorn University

Thesis Title	SYNTHESIS OF HYDROCARBONS FROM METHANOL OVER COBALT-BASED CATALYSTS
By	Miss Le Thi Ngoc Huyen
Field of Study	Chemical Technology
Thesis Advisor	Assistant Professor Prasert Reubroycharoen, D.Eng.
Thesis Co-Advisor	Rujira Jitrwung, Ph.D.

---

Accepted by the Faculty of Science, Chulalongkorn University in Partial  
Fulfillment of the Requirements for the Master's Degree

.....Dean of the Faculty of Science  
(Associate Professor Polkit Sangvanich, Ph.D.)

#### THESIS COMMITTEE

.....Chairman  
(Associate Professor Kejvalee Pruksathorn, Dr. de L'INPT)

.....Thesis Advisor  
(Assistant Professor Prasert Reubroycharoen, D.Eng.)

.....Thesis Co-Advisor  
(Rujira Jitrwung, Ph.D.)

.....Examiner  
(Professor Tharapong Vitidsant, Dr.de L'INPT)

.....External Examiner  
(Assistant Professor Chantip Samart, D.Eng.)

เล อี งอค เอ็อน : การสังเคราะห์ไฮโดรคาร์บอนจากเมทานอลบนตัวเร่งปฏิกิริยาฐานโคบอลต์ (SYNTHESIS OF HYDROCARBONS FROM METHANOL OVER COBALT-BASED CATALYSTS) อ.ที่ปรึกษาวิทยานิพนธ์หลัก: ผศ. ดร. ประเสริฐ เรียบร้อยเจริญ, อ.ที่ปรึกษาวิทยานิพนธ์ร่วม: ดร.รุจิรา จิตรหวัง, 56 หน้า.

งานวิจัยนี้ศึกษาการเปลี่ยนเมทานอลเป็นไฮโดรคาร์บอนโดยใช้โคบอลต์เป็นตัวเร่งปฏิกิริยา โดยสนใจศึกษาสภาวะของปฏิกิริยาต่อร้อยละการเปลี่ยนไปของสารตั้งต้นและค่าการเลือกเกิดเป็นผลิตภัณฑ์ในเครื่องปฏิกรณ์แบบกะและเครื่องปฏิกรณ์แบบเบดนิ่งขนาดใหญ่ และใช้โคบอลต์บนตัวรองรับอะลูมินาเป็นตัวเร่งปฏิกิริยา นอกจากนี้ยังได้ศึกษาผลของตัวเร่งปฏิกิริยาโคบอลต์บนตัวรองรับ 2 ชนิด คือ อะลูมินา และ ZSM-5 โดยทำการศึกษาในเครื่องปฏิกรณ์แบบเบดนิ่งขนาดเล็ก สำหรับในการศึกษาการเปลี่ยนเมทานอลเป็นไฮโดรคาร์บอนในเครื่องปฏิกรณ์แบบกะ พบว่าร้อยละการเปลี่ยนไปของสารตั้งต้นและร้อยละผลได้ของผลิตภัณฑ์สูงสุดเมื่อใช้ปริมาณตัวเร่งปฏิกิริยาร้อยละ 2 เมื่อทำการทดลองที่ภายใต้ความดัน 10 บาร์ ตัวเร่งปฏิกิริยาโคบอลต์บนตัวรองรับอะลูมินาให้ผลิตภัณฑ์ที่เป็นสารประกอบไฮโดรคาร์บอนสายโซ่ยาว และการทำปฏิกิริยาที่อุณหภูมิสูงและอัตราการไหลผ่านของสารตั้งต้นที่ต่ำกว่าทำให้เกิดปฏิกิริยาการแตกสลาย นอกจากนี้ตัวเร่งปฏิกิริยาโคบอลต์บนตัวรองรับ ZSM-5 ให้ค่าร้อยละการเปลี่ยนไปของสารตั้งต้นและร้อยละผลได้ของผลิตภัณฑ์ที่สูงกว่าตัวเร่งปฏิกิริยาที่รองรับด้วยซิลิกาและอะลูมินา ปริมาณของโลหะโคบอลต์บนตัวรองรับที่มากขึ้นส่งผลให้ร้อยละการเปลี่ยนไปของสารตั้งต้นลดลง นอกจากนี้ได้ศึกษาการนำตัวเร่งปฏิกิริยาโคบอลต์บนตัวรองรับอะลูมินามาใช้ร่วมกับ ZSM-5 เพื่อเป็นการเพิ่มประสิทธิภาพของตัวเร่งปฏิกิริยา การใช้ตัวเร่งปฏิกิริยาทั้ง 2 ชนิดร่วมกันโดยการแยกเบดของตัวเร่งปฏิกิริยาทั้ง 2 ชนิด และให้สารตั้งต้นผ่าน ZSM-5 ก่อน พบว่าวิธีการนี้ให้ค่าร้อยละการเปลี่ยนไปของสารตั้งต้นสูงสุด และให้ค่าการเลือกเป็นไฮโดรคาร์บอนที่มีคาร์บอนมากกว่า 7 อะตอมขึ้นไปที่ดีกว่า แต่ยังคงสูงกว่าการใช้ ZSM-5 เป็นตัวเร่งปฏิกิริยา

ภาควิชา	เคมีเทคนิค	ลายมือชื่อนิสิต	.....
สาขาวิชา	เคมีเทคนิค	ลายมือชื่อ อ.ที่ปรึกษาหลัก	.....
ปีการศึกษา	2558	ลายมือชื่อ อ.ที่ปรึกษาร่วม	.....

# # 5672208023 : MAJOR CHEMICAL TECHNOLOGY

KEYWORDS: METHANOL TO HYDROCARBON / COBALT CATALYST / ALUMINA / ZSM-5

LE THI NGOC HUYEN: SYNTHESIS OF HYDROCARBONS FROM METHANOL OVER COBALT-BASED CATALYSTS. ADVISOR: ASST. PROF. PRASERT REUBROYCHAROEN, D.Eng., CO-ADVISOR: RUJIRA JITRWUNG, Ph.D., 56 pp.

The research aims to study the conversion of methanol to hydrocarbon over cobalt-based catalyst. The effect of reaction condition on conversion and hydrocarbon selectivity was investigated in batch as well as large scale fixed-bed reactor by using Co/ $\gamma$ -Al<sub>2</sub>O<sub>3</sub>. In addition, the catalytic activity of Co supported on various carriers and combination between ZSM-5 and Co/ $\gamma$ -Al<sub>2</sub>O<sub>3</sub> was studied in small scale fixed-bed reactor. In batch reactor, the conversion and yield of total hydrocarbon product using 2% catalyst was reached maximum over catalyst loading of 3% for 2h at 300°C. The catalytic performance of Co/ $\gamma$ -Al<sub>2</sub>O<sub>3</sub> catalyst exhibited the long chain hydrocarbon at 10bar. Over Co/ $\gamma$ -Al<sub>2</sub>O<sub>3</sub>, the higher temperature and lower flow rate favored cracking reaction. Furthermore, ZSM-5 supported Co obtained high conversion as well as yield of hydrocarbon. The loading of cobalt is negative effect on methanol conversion. To improve the catalytic activity of Co/ $\gamma$ -Al<sub>2</sub>O<sub>3</sub> by combining with ZSM-5. The separated beds in order of ZSM5 and Co/ $\gamma$ -Al<sub>2</sub>O<sub>3</sub> reached highest methanol conversion in different combination ways. However, it is lower selectivity towards C<sub>7</sub><sup>+</sup> hydrocarbon but higher by product selectivity than ZSM-5.

Department: Chemical Technology      Student's Signature .....

Field of Study: Chemical Technology      Advisor's Signature .....

Academic Year: 2015      Co-Advisor's Signature .....

## ACKNOWLEDGEMENTS

I would never be able to complete my thesis without the guidance of committee member, help from my friends, and support from my family.

I would like to express her gratitude to advisor, Asst. Prof. Dr. Prasert Reubroychroen and co-advisor, Dr. Rujira Jitwung for their encouraging guidance, advice and suggestion throughout this research. I also would like to acknowledge, Assoc. Prof. Dr. Kejvalee Pruksathorn, Prof. Dr. Tharapong Vitidsant, and Asst. Prof. Chanatip Samart for serving as chairman and members of thesis committee, respectively.

I would like to thank Thailand Institute of Scientific and Technological Research (TISTR) and Scholarship Program for ASEAN Countries, Chulalongkorn University for financial support of this research.

Finally, I thank all people in the Department of Energy Technology, Thailand Institute of Scientific and Technological Research and Department of Chemical Technology, Faculty of Science, Chulalongkorn University for helping me to characterize catalyst and use equipments.

## CONTENTS

	Page
THAI ABSTRACT .....	iv
ENGLISH ABSTRACT .....	v
ACKNOWLEDGEMENTS .....	vi
CONTENTS .....	vii
LIST OF TABLES .....	1
LIST OF FIGURES .....	2
LIST OF ABBREVIATION.....	4
CHAPTER I INTRODUCTION.....	6
1.1. Statement of problem .....	6
1.2. Scope of research .....	7
1.3. Objective .....	7
CHAPTER II THEORY AND LITERATURE REVIEW .....	8
2.1 Methanol to hydrocarbon process .....	8
2.2. Reaction mechanism for MTH process .....	9
2.3. Catalysts for methanol to hydrocarbons .....	11
2.3.1. Zeolitic catalyst.....	12
2.3.2. Nonzeolitic catalyst .....	13
2.3.3. Deactivation .....	14
2.4. Cobalt-based catalyst.....	14
2.5. Literature review.....	17
CHAPTER III EXPERIMENTAL.....	19
3.1 Materials.....	19

	Page
3.2 Characterization of catalysts.....	19
3.2.1. Nitrogen adsorption-desorption measurement .....	19
3.2.2. X-ray diffraction (XRD).....	20
3.2.3. Temperature-programmed desorption of $\text{NH}_3$ ( $\text{NH}_3$ -TPD).....	20
3.2.4. Temperature-programmed reduction of $\text{H}_2$ ( $\text{H}_2$ -TPR) .....	20
3.2.5. Thermogravimetric analysis (TGA) .....	21
3.3. Catalyst preparation .....	21
3.4. Catalyst reduction .....	22
3.5. The catalytic apparatus.....	22
3.5.1. Batch reactor .....	22
3.5.2. Fixed-bed reactor.....	23
3.5.2.1. Larger scale.....	23
3.5.2.2. Small scale.....	24
3.5.2.3. Product analysis.....	25
CHAPTER IV RESULTS AND DISCUSSION .....	27
4.1. Characterization of catalysts.....	27
4.1.1. Nitrogen adsorption-desorption.....	27
4.1.2. X-ray diffraction .....	27
4.1.3. Temperature-programmed desorption ( $\text{NH}_3$ -TPD).....	28
4.1.4. Temperature-programmed reduction ( $\text{H}_2$ -TPR).....	29
4.2. The catalytic activity of cobalt-based catalyst .....	30
4.2.1. Batch reactor .....	30
4.2.1.1. Effect of reaction time.....	30



	Page
4.2.1.2. Effect of catalyst weight percent .....	32
4.2.2. Large scale fixed-bed reactor .....	33
4.2.2.1. Effect of temperature .....	33
4.2.2.2. Effect of pressure .....	35
4.2.2.3. Effect of feed flow rate .....	36
4.2.3. Small scale fixed-bed reactor .....	37
4.2.3.1. Effect of support .....	37
4.2.3.2. Effect of cobalt loading .....	39
4.2.3.3. Effect of separated or mixed beds of Co/ $\gamma$ -Al <sub>2</sub> O <sub>3</sub> and ZSM-5 .....	40
4.2.3.4. Effect of temperature over separated beds of catalysts in order ZSM-5 and Co/ $\gamma$ -Al <sub>2</sub> O <sub>3</sub> .....	43
4.3. Stability of catalyst .....	46
CHAPTER V CONCLUSIONS AND RECOMMENDATIONS .....	48
5.1 Conclusions .....	48
5.2 Recommendations .....	49
REFERENCES .....	50
APPENDIX .....	53
VITA .....	56

## LIST OF TABLES

Table 1: List of chemicals and source .....	19
Table 2: Textual properties and $\text{Co}_3\text{O}_4$ crystallite size ( $d_{\text{Co}_3\text{O}_4}$ ) of support and catalyst.....	27
Table 3: The effect of reaction time on methanol conversion and product distribution .....	31
Table 4: Effect of catalyst weight percent on methanol conversion and product distribution .....	32
Table 5: Effect of temperature on methanol conversion and hydrocarbon distribution .....	34
Table 6: Effect of pressure on methanol conversion and product distribution.....	35
Table 7: Effect of feed flow rate on methanol conversion and product distribution .....	36
Table 8: Effect of support on methanol conversion and product distribution.....	38
Table 9: Effect of cobalt loading.....	39
Table 10: Effect of separated or mixed beds of $\text{Co}/\gamma\text{-Al}_2\text{O}_3$ and ZSM-5.....	40
Table 11: Effect of temperature over separated beds of catalysts in order ZSM-5 and $\text{Co}/\gamma\text{-Al}_2\text{O}_3$ .....	44

## LIST OF FIGURES

Figure 1: Simplified representation of the different pathways for methanol conversion [4].....	9
Figure 2: Schematic of temperature-program of TPD .....	20
Figure 3: Schematic of temperature-program of TPR .....	21
Figure 4: Schematic diagram of batch reactor.....	23
Figure 5: Schematic diagram of fixed-bed reactor.....	24
Figure 6: Schematic diagram of small scale fixed-bed reactor .....	25
Figure 7: The GC heating program for gas analysis.....	25
Figure 8: The GC heating program for gas analysis.....	26
Figure 9: The GC-MS program for liquid analysis .....	26
Figure 10: XRD patterns of ZSM-5, Co/ZSM-5, Co/SiO <sub>2</sub> , and Co/ $\gamma$ -Al <sub>2</sub> O <sub>3</sub> catalysts .....	28
Figure 11: NH <sub>3</sub> -TPD profiles of ZSM-5 and Co-based catalysts .....	29
Figure 12: H <sub>2</sub> -TPR pattern of Co-based catalysts .....	30
Figure 13: Effect of reaction time on product distribution in (a) gaseous phase and (b) liquid phase; reaction condition: 63g of methanol, 0.63g of Co/ $\gamma$ -Al <sub>2</sub> O <sub>3</sub> , 1 bar initial pressure of N <sub>2</sub> , 300°C.....	32
Figure 14: Effect of catalyst weight percent on product distribution in (a) gaseous phase and (b) liquid phase; reaction condition: 63g of methanol, Co/ $\gamma$ -Al <sub>2</sub> O <sub>3</sub> , 1 bar initial pressure of N <sub>2</sub> , 300°C, 2h reaction time. ....	33
Figure 15: Effect of temperature on product distribution.....	35
Figure 16: Effect of pressure on product distribution .....	36
Figure 17: Effect of feed flow rate on product distribution.....	37
Figure 18: Effect of support on product distribution .....	39

Figure 19: Effect of separated or mixed beds of Co/ $\gamma$ -Al <sub>2</sub> O <sub>3</sub> and ZSM-5 on product distribution in (a) C <sub>2</sub> – C <sub>6</sub> and (b) C <sub>7</sub> <sup>+</sup> hydrocarbon product (T = 400°C, P= atm, F <sub>MeOH</sub> = 0.1ml/min, 1g of catalyst, Co/ $\gamma$ -Al <sub>2</sub> O <sub>3</sub> : ZSM-5 = 1:1).....	41
Figure 20: Effect of separated or mixed beds of Co/ $\gamma$ -Al <sub>2</sub> O <sub>3</sub> and ZSM-5 on product distribution in product weight percent (T = 400°C, P= atm, F <sub>MeOH</sub> = 0.1ml/min, 1g of catalyst, Co/ $\gamma$ -Al <sub>2</sub> O <sub>3</sub> : ZSM-5 = 1:1).....	43
Figure 21: Effect of temperature on product distribution over separated beds of catalysts in order ZSM-5 and Co/ $\gamma$ -Al <sub>2</sub> O <sub>3</sub> in (a) C <sub>2</sub> – C <sub>6</sub> and (b) C <sub>7</sub> <sup>+</sup> hydrocarbon product (P= atm, F <sub>MeOH</sub> = 0.1ml/min, ZSM-5 : Co/ $\gamma$ -Al <sub>2</sub> O <sub>3</sub> = 1:1, 1g of catalyst).....	45
Figure 22: Effect of temperature on product distribution in product weight percent over separated beds of catalysts in order ZSM-5 and Co/ $\gamma$ -Al <sub>2</sub> O <sub>3</sub> (P= atm, F <sub>MeOH</sub> = 0.1ml/min, ZSM-5 : Co/ $\gamma$ -Al <sub>2</sub> O <sub>3</sub> = 1:1, 1g of catalyst).....	45
Figure 23: TGA profile of spent catalyst.....	47
Figure 24: XRD pattern of spent catalysts .....	47
Figure 25: XRD pattern of Co/ $\gamma$ -Al <sub>2</sub> O <sub>3</sub> .....	54

## LIST OF ABBREVIATION

Co	Cobalt
SiO <sub>2</sub>	Silicon dioxide (silica)
γ-Al <sub>2</sub> O <sub>3</sub>	Gamma alumina
ZSM-5	Zeolite Socony Mobil-5
MCM	Mobil Composition of Matter No.41
SHS	Silica hollow sphere
CO	Carbon monoxide
CO <sub>2</sub>	Carbon dioxide
CH <sub>4</sub>	Methane
DME	Dimethyl ether (CH <sub>3</sub> OCH <sub>3</sub> )
N <sub>2</sub>	Nitrogen
H <sub>2</sub>	Hydrogen
He	Helium
NH <sub>3</sub>	Amonia
wt.%	Weight percent
wt.	Weight
mol.%	Carbon mole percent
T	Temperature
P	Pressure
°C	Degree Celsius
K	Degree Kelvin
XRD	X-ray Diffraction
TPR	Temperature-programmed reduction
TPD	Temperature-programmed desorption
TGA	Thermogavimetric analysis
GC	Gas chromatograph
GC-MS	Gas chromatograph-mass spectrometry
TCD	Thermal conductivity detector

FID	Flame ionization detector
FTS	Fischer Tropsch synthesis
MTH	Methanol to Hydrocarbons
MTO	Methanol to olefin
MTG	Methanol to gasoline
MOGD	Mobil Olefin to Gasoline and Distillation
$F_{\text{MeOH}}$	Flow rate of methanol
SAPO	Silicoaluminophosphate
atm	Atmospheric pressure
$\mu\text{m}$	Micron meter
$\text{cm}^3$	cubic centimeter
ml	Mililiter
min	Minute (s)
g	gram (s)
et.al	and others



## CHAPTER I

### INTRODUCTION

#### 1.1. Statement of problem

Liquid fuel is a significant factor for transportation and economics. The conventional production of liquid fuel is based on petroleum sources and crude oil obtained not only generates air pollution but also sometimes hazards to water public area where oil is leakage. Moreover, the shortage of oil is widely recognized and it becomes the common problems of the world. In this situation, the synthetic fuel obtained from green sources is interesting.

Nowadays, synthetic liquid fuel can be obtained from alternative processes. Liquid fuel can be converted indirect from coal, natural gas or biomass via synthetic gas (the mixture of carbonmonoxide and hydrogen). Methanol is widely known as a chemical previously produced from coal, natural gas. Nevertheless, it is classified as a green chemical when it is obtained from biomass but not limited to synthetic gas route also fermentation process. Although methanol itself is the potential motor fuel or blended with gasoline, it would demand large investments to innovate motors to use methanol directly as fuel. Alternatively, methanol can be converted to hydrocarbon such as high octane gasoline or plastic monomers depending on an appropriate catalyst and operation condition.

Methanol to hydrocarbons have been attracted the researchers continuously. The scientists have focused on the production of hydrocarbons in gasoline range or plastic monomer from methanol. However, the demand for other kinds of fuel is increased rapidly, such as jet fuel or diesel. Alternatively, the synthetic diesel can be produced by Fischer-Tropsch process from syngas. The cobalt-based catalysts are high selective catalysts for Fischer-Tropsch process towards to diesel fraction.

This research will focus on developing the catalysts for conversion methanol to long chain hydrocarbon ( $C_7^+$ ). Moreover, the catalytic performance of the catalysts will be studied.

## 1.2. Scope of research

The experimental procedures was carried out as follows

1. Prepare cobalt catalyst by incipient impregnation method.
2. Investigate the effect of reaction condition on methanol conversion and hydrocarbon yield in batch reactor
3. Investigate the effect of reaction condition on methanol conversion and hydrocarbon yield in fixed-bed reactor
4. Analyze the gas and liquid products by gas chromatograph (GC) and gas chromatograph-mass spectrometry (GC-MS).
5. Characterize catalysts as follows
  - Nitrogen adsorption isotherm (BET)
  - X-ray diffraction (XRD)
  - Temperature-programmed desorption ( $\text{NH}_3$ -TPD)
  - Temperature-programmed reduction ( $\text{H}_2$ -TPR)
  - Thermogravimetric analysis (TGA)
6. Summarize the result and write thesis.

## 1.3. Objective

- To prepare cobalt-based catalysts by impregnation method.
- To study the effects of catalyst for synthesizing long chain hydrocarbons from methanol.



## CHAPTER II

### THEORY AND LITERATURE REVIEW

#### 2.1 Methanol to hydrocarbon process

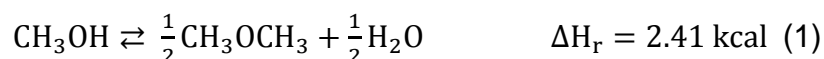
Methanol is a feedstock of synthetic fuel processes such as dimethyl ether, gasoline or diesel. Dimethyl ether might replace liquefied petroleum gas (LPG) and diesel in the future because its properties are high thermal energy as LPG and equivalent to cetane number of diesel. On the other hand, hydrocarbons, which are the composition of synthetic fuel, were produced from methanol. Since 1970s, the Mobil workers discovered that an acidic zeolite called ZSM-5 (Zeolite Socony Mobil-5) was able to catalyze the practical conversion of methanol to both olefins and hydrocarbons in gasoline range. The methanol to gasoline (MTG) processes generates gasoline consisting of  $C_1$  to  $C_{11}$  hydrocarbons with 80% of  $C_5^+$  selectivity. The compositions of gasoline are paraffins, olefins, aromatics and naphthenes are obtained when applied under 20 bar pressure and carried out at temperature range of 350-400°C for the MTG process [1].

In addition, olefins obtained from methanol to olefin (MTO) process are not only polymeric monomer but also intermediate product of Olefins to Gasoline and Distillation (MOGD) process. MOGD process as a refinery process was also developed by Mobil. In this process, the olefins from the MTO unit are oligomerized over a ZSM-5 catalyst to hydrocarbons in the gasoline and/ or distillation range. The ratio between gasoline and distillate can be varied considerably depending on the reaction conditions to allow a significant flexibility in production. The distillate mode is defined when the operating condition is low temperature and high pressure (200-300°C, 20-105 bar). The products of distillate mode process are high molecular weight olefins, which are hydrogenated to produce fuel including diesel and premium quality jet fuels. Conversely, the operating condition is changed to higher temperature and lower pressures that led to formation of lower molecular weight products with higher aromatic content (i.e., high-octane gasoline) [2].

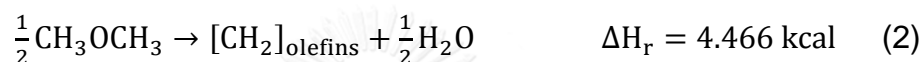
## 2.2. Reaction mechanism for MTH process

The methanol to hydrocarbon reaction is highly exothermic and the heat of reaction is 10.69 (kcal/kg of methanol). The conversion of methanol to hydrocarbons can be represented by the following sequence of steps [3]

Step 1: Methanol is dehydrated to dimethyl ether (DME).



Step 2: The equilibrium mixture is formed consisting of methanol, dimethyl ether and water, then converted to light olefins.



Step 3: In the last step, the light olefins is reacted to form paraffins, aromatics, naphthenes, and higher olefins by hydrogen transfer alkylation and polycondensation.



The reaction mechanism of methanol to hydrocarbon has been the topic of various studies. The formation of first C-C bond from C<sub>1</sub> units, such as methanol or dimethyl ether, was available displayed more than 20 possible mechanistic proposals. The reaction pathway, which shows how to obtain classes of hydrocarbons from methanol, is exhibited in Figure 1.

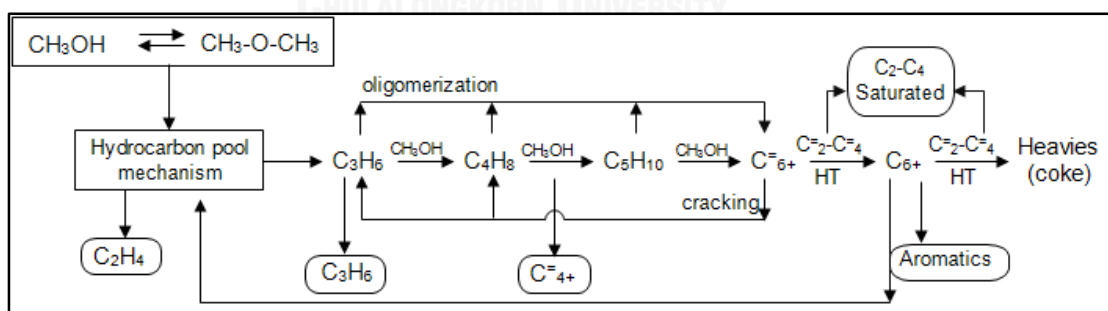
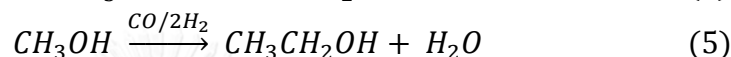


Figure 1: Simplified representation of the different pathways for methanol conversion [4]

The reaction pathway for methanol conversion is called “hydrocarbon pool” (HP) mechanism. The primary hydrocarbons are the most probably the lower olefins, like ethylene and propylene. On the pathways, the formation of C<sub>4</sub>, C<sub>5</sub> and C<sub>6</sub><sup>+</sup> olefins

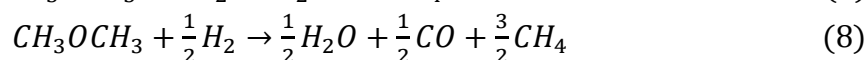
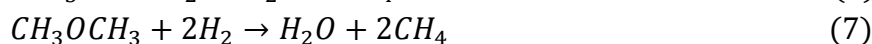
can be transferred from the primary hydrocarbons, especially propylene. The  $C_6^+$  aliphatic species can produce either aromatics, heavy carbonaceous concurrently with the formation of saturated light hydrocarbon by hydrogen transfer (HT) reactions or propylene, butane by cracking process.

In the Fischer-Tropsch process, the hydrogenation of CO over cobalt catalyst form linear alkanes. Small amount of CO, which is decomposed from methanol, is detected in MTH gas products. In MTH mechanism, CO is proposed to be either an intermediate or co-catalyst. [5]

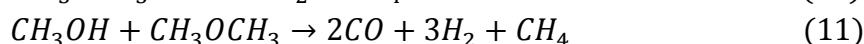
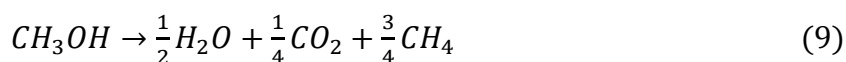


Methane, which are formed continuously during MTH process, is the by-product. There are some paths of methane formation. The hydrogenolysis reactions of methanol and DME to methane were favored at low temperature as shown in equation 6 to 8. The decomposition of methanol and DME were the predominant route of methane formation at high temperature as shown in equation 9 to 11. The other way was the demethylation of aromatics as shown in equation 12 to 14. In addition, the formation of methane can be obtained when the process conditions are applied at high temperature, high flow rate of feed, low pressure, and weak acid sites. The following reactions of methane formation are shown [6]

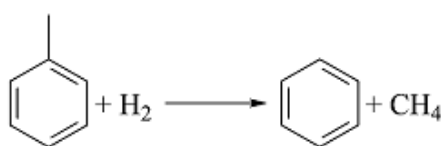
Hydrogenolysis of methanol and DME

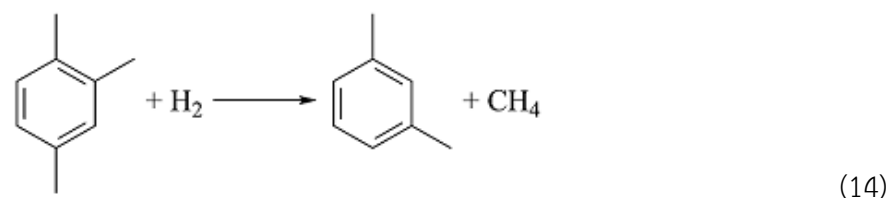
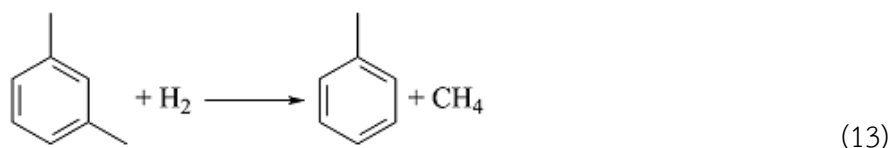


Decomposition of methanol and DME



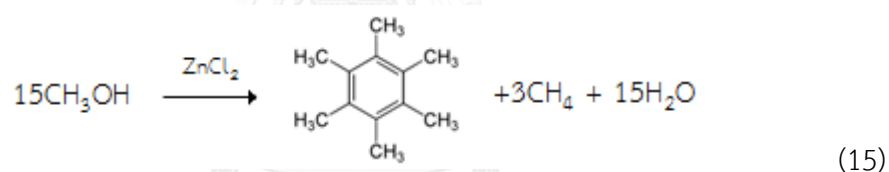
Demethylation of aromatics





### 2.3. Catalysts for methanol to hydrocarbons

Over a century ago, the discovery of hydrocarbon formed by adding some drops of methanol on zinc chloride methanol was firstly reported by LeBel and Greene. The products were hexamethylbenzene and gaseous saturated hydrocarbons, mostly  $\text{CH}_4$  as shown in equation 15.



Afterward the research studies on conversion methanol to hydrocarbons have been focused continuously. Some catalysts, such as zinc iodide, phosphorus pentoxide, polyphosphoric acid, and later tantalum pentafluoride and other super acid systems have been reported for the synthesis of hydrocarbons from methanol, but these catalysts are deactivated rapidly. Since 1970s, the Mobil workers discovered that an acidic zeolite called ZSM-5 (Zeolite Socony Mobil-5) was able to catalyze the practical conversion of methanol to both olefins and hydrocarbons in gasoline range [2]. The synthetic aluminosilicate zeolite, ZSM-5 has the MFI topology. ZSM-5 has 3-dimensional system of 10-atom rings channels, channel interconnecting, and pore opening. The researchers at UOP developed silicoaluminophosphate (SAPO) molecular sieve (such as SAPO-34 and SAPO-17) exhibit the high catalytic activity for MTO process

[2]. SAPO-34 has CHA structure, 3-dimensional channel of 8-atom ring channel, channel interconnecting, and pore opening of 3.8 Å [7].

The conversion of methanol to hydrocarbon depends on the catalytic properties, such as catalyst topology, crystallite size, acid strength, acid site density.

### 2.3.1. Zeolitic catalyst

Large pore zeolite has been found to catalyze methanol conversion. Faujasite, mordenite, mazzite (ZSM-4) were defined 12-ring windows. The selectivity toward olefin was studied over Faujasite by applying Ni, Cr and Pb exchanged Ca-Y zeolites, incorporation of Cr and Pb into NiCa-Y zeolite, rare-earth and Zn-exchanged X-type zeolite [8]. The catalyst was deactivated rapidly over large pore zeolite. It can be reduced by catalyst modification, such as metal-exchanged faujasite [9]. The various cations exchange mordenite improved C<sub>1</sub>-C<sub>5</sub> hydrocarbon yield at 350-500°C [9]. Dealumination of mordenite not only enhanced the activity but also resisted the deactivation in MTG process [8].

ZSM-5, which is medium pore zeolite with 10-ring windows, has usually applied for methanol conversion. A number of papers were published the application of ZSM-5 for MTO or MTG process. When applying ZSM-5 at 371°C, the main products are isoparaffins and aromatics. Because of shape selectivity of zeolite, the narrow range of hydrocarbon is about C<sub>10</sub> [9]. Light olefin can be produced from methanol over ZSM-5 zeolite by controlling reaction condition as well as catalyst preparation. The high selectivity toward olefin can be obtained at higher temperature, longer space time, lower pressure of methanol and dimethyl ether. The synthesis conditions of ZSM-5, including sodium-free gels, crystallization time, crystal size less than 2µm affect significantly on production of high olefin selectivity [8]. Furthermore, the structure of medium (ZSM-5) and large (ZSM-12) pore zeolite are suitable for oligomerization of olefin to long chain paraffin (C<sub>12</sub>-C<sub>20</sub>). In addition, SiO<sub>2</sub>/Al<sub>2</sub>O<sub>3</sub> in ZSM-5 zeolite did not significantly influenced to yield of diesel fraction [10]. Moreover, other medium pore catalysts have been investigated for methanol conversion. While ZSM-11 catalyzed methanol to aromatic product, ZSM-48 and EU-2 zeolite (high silica medium-pore zeolite) catalyzed methanol to olefins [10].

Small pore zeolite with 8-ring windows has high selectivity for synthesis of olefin such as ethylene and propene from methanol. Kaiser reported the high conversion methanol to olefin over SAPO molecular sieves, especially SAPO-17 and SAPO-34. The selectivity of olefin can be reached to about 96% over SAPO-34 while the yield of methane and saturated hydrocarbon were low at 375°C-450°C, atmospheric pressure. In addition, Kaiser used the mixture of water-methanol for converting to light olefins over metalloaluminophosphate (MeAPO) and methallosilicoaluminophosphate (MeAPSO). MgAPO-34, CoAPSO-34, and MnAPO-34 applied to convert methanol, but they were high selectivity to methane and carbon dioxide. The synthesis of olefin from methanol was presented by Chang over chabazite, erionite, zeolite T, and zeolite ZK-5. At 100% methanol conversion, the light hydrocarbon was less than 60 wt%. The yield of hydrocarbon obtained richer but methanol conversion dropped by modifying zeolite such as dealuminated H-erionite or chabazite [8].

### 2.3.2. Nonzeolitic catalyst

The types of catalyst can be classified as zeolite catalysts and nonzeolitic catalysts. Most of researchers have studied the conversion of methanol to hydrocarbon over zeolitic material. However, other catalysts were investigated the production of hydrocarbon from methanol. Dolgov reported that methanol converted to 2-4% ethane and dimethylether over  $\text{H}_2\text{SO}_4$  at 135-140°C [9]. The composition of 39.1-43%  $\text{Al}_2\text{O}_3$  plus  $\text{TiO}_2$ , 0.83-0.93% $\text{Fe}_2\text{O}_3$ , 0.15-0.3% $\text{Mg}$  and  $\text{CuO}$  deposited on clay pellets that was used for synthesizing ethene from DME at 100-150°C, 1-1.5 atm, and  $0.03\text{h}^{-1}$ . It was presented by Matyushenskii and Freidlin [9]. Kim et al. reported the conversion methanol to hydrocarbon over zinc iodide at 200°C. The products consisted of small amount of  $\text{C}_4$  hydrocarbon, gas oil range (230-270°C), gasoline range ( $\text{C}_5$ - $\text{C}_{15}$ ), and 2-3% heavier fraction with little solid residue [9]. Methanol converted to mainly olefinic product (20-60% yield of  $\text{C}_2$ - $\text{C}_4$  olefin) over alumina dihydrogenphosphate at 375-425°C. It was published by Kikkawa. Acid and several salts of 12-tungstophosphoric acid,  $\text{H}_3\text{PW}_{12}\text{O}_{40}$  were applied to study the conversion of methanol to hydrocarbon at 290°C. Ethylene, propylene and  $\text{C}_4^+$  hydrocarbon such as aromatics were formed over

$\text{H}_3\text{PW}_{12}\text{O}_{40}$ . Ehwald et al. showed the stability of catalytic activity over  $\text{Ag}_4(\text{SiW}_{12}\text{O}_{40})$ . Lanthanide modified  $\text{H}_3\text{PW}_{12}\text{O}_{40}$  synthesized high olefin selectivity at  $300^\circ\text{C}$ ,  $0.2\text{h}^{-1}$  [8]. Other catalysts, such as aluminum sulfate, silica alumina, tungsten oxide over alumina, heteropolyacids and salts of heteropolyacids catalyzed the methanol conversion to hydrocarbon [9]. Mesoporous silico-alumina applied for producing clean diesel fuel. Silico-aluminate MCM-41 with ratio Si/Al of 20 was used to oligomerize  $\text{C}_4$  and  $\text{C}_5$  to high diesel fraction [11].

### 2.3.3. Deactivation

The reason of catalyst deactivation during the MTH process is coking. The properties of catalyst and reaction condition, which are catalyst topology, crystal size, acid strength, acid density, and temperature, pressure affect to the deactivation rate and the nature as well as the amount of coke. According to Figure 1, heavy molecules like polycyclic aromatics were formed in the final stage of MTH mechanism over medium and large pore zeolite. The absorption on the active site and/or blocking the pore by these molecules lead to deactivate catalyst [4, 12]. On the contrary, the coke on low acidic ZSM-5 is mainly mono- or bi-aromatic which does not influence significantly on catalytic activity [12].

### 2.4. Cobalt-based catalyst

Cobalt-based catalysts are especially interesting from the commercial catalysts because of their rather high activity and selectivity with respect to linear hydrocarbons. Generally, cobalt-based catalyst is used for Fischer-Tropsch process which is the hydrogenation of carbon monoxide to liquid fuels. Cobalt, which is the transition metal, is ability to catalyze the chemical reaction. Cobalt are usually dispersed on high-surface area supports stable such as  $\text{Al}_2\text{O}_3$ ,  $\text{TiO}_2$ , or  $\text{SiO}_2$  due to high price of cobalt and improved stability of catalyst.

The interaction between cobalt and support affects to dispersion of cobalt. The strong interaction between support and cobalt precursor lead to high dispersion cobalt. However, the strong interaction required high reduction temperature that forms

the large cobalt particles. On the contrary, when cobalt precursor and support interact weakly, the cobalt precursors are reduced easily but they are not stable during drying step. Therefore, the intermediate interaction strength facilitated to obtain the optimum cobalt dispersion [13].

The supports impact greatly on activity of Co-based catalysts. The properties of support are high melting point, stable under reaction condition, high surface area, and porous structure. The porosity of support can manage the size of metal and oxide species and reduction. It was studied over mesoporous silica MCM-41 with diameter range of 20-330 Å. The increase in pore size of support broaden the cobalt oxide particle. The reduction of Co oxide particle located in the narrow pore (20-50 Å) is more difficult than that in the wide pore (>50Å) [14].

Alumina supported catalyst: Alumina is the common support because of high thermal stability and catalytic properties, such as wide range of surface area, pore size, surface acidity. It can be classified by transitional phases  $\beta$ ,  $\gamma$ ,  $\eta$ ,  $\chi$ ,  $\kappa$ ,  $\delta$ ,  $\theta$ , and  $\alpha$ -Al<sub>2</sub>O<sub>3</sub>. Rane et al. [15] studied that the interaction between alumina phase ( $\delta$ -,  $\theta$ -,  $\alpha$ -, and  $\gamma$ -Al<sub>2</sub>O<sub>3</sub> support) and cobalt particles were not effect on cobalt metal dispersion. The amount of ethylene glycol and deionized water in impregnation solution governed the cobalt particle size. However, in FTS, the C<sub>5</sub><sup>+</sup> selectivity over  $\delta$ ,  $\alpha$ -Al<sub>2</sub>O<sub>3</sub> support was higher than that over  $\theta$ -,  $\gamma$ -Al<sub>2</sub>O<sub>3</sub> support. Promoter platinum favored to narrow Co<sub>3</sub>O<sub>4</sub> crystallite size and cobalt particle size in catalyst reduction [16]. Calcium oxide promoted the Co oxide reducibility, and decreased the formation of cobalt-aluminate species which were hard to reduce to Co metal [17]. Calcination temperature range of 473-773K did not significantly impact on Co<sub>3</sub>O<sub>4</sub> crystallite size but exhibited the harder reducibility at higher temperature [16]. Alumina can be deactivated by the presence of water in MTH process. The absorption of water on surface leads to loss of active site and compete with methanol absorption [18].



Silica-support catalyst: Silica is used as a support in industrial application due to high surface area. However, it is low thermal stability in comparison with  $\text{Al}_2\text{O}_3$ . Girardon et al. [19] reported the effect of cobalt precursor and catalyst pretreatment on cobalt reducibility. The endothermic decomposition of cobalt nitrate was favorable to  $\text{Co}_3\text{O}_4$  while the exothermic decomposition of cobalt acetate was preferable to cobalt silicate, which was hard to transform to active sites after reduction. The dispersion of cobalt oxide on support favored at low temperature of cobalt nitrate decomposition and calcination. Ruthenium promoter not only enhanced cobalt reducibility but also decreased in cobalt silicate species.

Zeolite supported catalyst: Zeolite or crystallite aluminosilicates is porous structure. Zeolite is used as catalyst or support for petroleum refining, chemical manufacture, conversion of coal or natural gas process. ZSM-5 supported Co leads to reduce the total density of acid sites due to blocking acid site by cobalt. The strong interaction between Co and ZSM-5 formed more Co particles with lower coordination sites [20]. Satipi et al. [21] studied the acid-catalyzed reaction for converting n-hexane and  $\text{H}_2$  to hydrocarbon compound over zeolite supports and supported Co-catalyst. The conversion over Co/H-ZSM-5 was higher than that over Co/ $\text{SiO}_2$  because of higher hydrogenolysis activity. Acid sites in vicinity with Co facilitated to acid-catalyzed reaction, such as cracking or isomerization. The selectivity toward hydrocarbons in gasoline range over Co/ZSM-5 was higher than that conventional catalyst (Co/ $\text{SiO}_2$ ) due to hydrocracking of primary FTS hydrocarbon [21]

The cobalt-based catalysts are deactivated by many reasons. There are poisoning, sintering of cobalt crystallites, interaction between metal and support. Cobalt-based catalyst is easily poisoned by the appearance of sulfur or nitrogen compound. Sintering can be caused by two major mechanisms, such as migration of atomic or crystallite cobalt. The possibility of sintering for exothermic reaction is rather high. Rønning et al. studied the change in cobalt crystallite during FTS reaction by

synchrotron XRD diffraction. In fixed-bed reactor, the poor heat transfer rose temperature during reaction. The increase in temperature to 400°C led to sinter cobalt crystals. The presence of water was caused sinter cobalt crystallite [22].

## 2.5. Literature review

Olefins are the immediate products for synthesis of long chain hydrocarbons from methanol. Some researchers studied the effect of catalysts and reaction conditions on the conversion methanol to olefins. Park et al. [23] studied the effects of the pore structure and acidity of zeolites on their product distribution and deactivation rates in the methanol-to-olefin reaction with different topologies of CHA, LTA, MFI, BEA, MOR and FAU zeolites. In the research, CHA, LTA zeolite with small pore opening showed high selectivity for lower olefins, while MFI, FAU and BEA zeolite with large pore opening showed high selectivity for alkylaromatics. The partially blocked pores of MOR zeolite showed high selectivity for lower olefins. The pore structure of zeolite strongly influenced their deactivation rate in the methanol-to-olefin reaction. The large cages of LTA and FAU zeolites deactivated rapidly because they allowed the methylbenzenes to condense continuously to polycyclic aromatic hydrocarbon. Although MOR zeolite with the linear pore structure inhibited any further condensation, the blocking pore by a few polycyclic aromatic hydrocarbons caused rapid deactivation.

Hajimirzaee et al. [24] investigated the effect of reaction parameters (temperature, pressure, weight hourly space velocity and feed composition) on the catalytic performance of methanol dehydration to olefin over H-ZSM-5 catalyst. Methanol conversion was increased when the temperature rose from 340°C to 400°C, but the conversion then dropped at higher temperature. The temperature at 400°C was suitable to produce more selectively light olefins. The selectivity towards  $C_5^+$  did not change in the range of 340 – 380°C, but went down when the temperature went up from 380°C to 460°C. The pressure in range of 1 to 20 bars, the selectivity of heavier hydrocarbons ( $C_5^+$ ) increased slowly and the selectivity to light olefins decreased. High space velocity led to produce more light olefins, despite the reduction in methanol

conversion. The researchers also studied the effect of different ratios of  $\gamma\text{-Al}_2\text{O}_3$  as a support to zeolite. 25% of ZSM-5 supported on  $\gamma\text{-Al}_2\text{O}_3$  produced light olefin more selective than other ratios but faster deactivation.

Riad et al. [25] studied the conversion of methanol to hydrocarbons over cobalt (4 wt.%) /  $\gamma\text{-Al}_2\text{O}_3$  and cobalt (4 wt.%) – lanthanum (2,4,6 wt.%) /  $\gamma\text{-Al}_2\text{O}_3$  catalysts in the micro-reactor. They focused on the effect of active sites on the catalytic activity and hydrocarbons selectivity. They found the conversion of methanol to aromatics mounted up as the increase in lanthanum loading which showed that the active sites of  $\text{LaCoO}_3$  and  $\text{La}_2\text{O}_3$  over  $\gamma\text{-Al}_2\text{O}_3$  is necessary for aromatic formation. They also studied the effect of temperature on hydrocarbon formation. The selectivity for alkane hydrocarbons formation reduced with the rise in reaction temperature range of 250-300°C.

The catalytic performance in Fischer – Tropsch synthesis depended on the cobalt particle size and support structure, which caused by the amount of cobalt loading, pore diameter, pore size distribution. It is shown in the following literature. Zeng et al. [26] studied the effect of cobalt loading and support pore structure on the selective diesel fraction in Fischer – Tropsch synthesis. SBA-16, which was used in this research, was a highly effective support to disperse cobalt species. When the cobalt loading went up (10, 15, 20 wt.%), the  $\text{Co}^\circ$  active site rose but the  $\text{Co}^\circ$  dispersion declined. An increase in cobalt loading led to high CO conversion and high  $\text{C}_5^+$  hydrocarbon selectivity, and especially high selectivity towards the diesel fraction.

Borg et al. [27] focused on the pore size of  $\gamma\text{-Al}_2\text{O}_3$  supported cobalt catalyst and Re-promoted cobalt catalyst in Fischer – Tropsch synthesis. The  $\text{C}_5^+$  selectivity strongly increased with larger pore diameter. Re promoter enhanced the reducibility of cobalt supported on  $\gamma\text{-Al}_2\text{O}_3$ , cobalt dispersion and, therefore, the catalytic activity. Re also raised the  $\text{C}_5^+$  selectivity. While Re affected strongly on catalytic performance of narrow-pore-based catalyst, the effect was smaller for wide-pore-based-catalyst.

Jung et al. [28] investigated the catalytic performance of cobalt – based catalyst supported on different mesoporous silica ( $\text{SiO}_2$ , MCM-41, periodic mesoporous silica hollow sphere (SHS)). The Co/SHS catalyst showed higher catalytic performance and  $\text{C}_5^+$  selectivity than other catalysts due to unique pore structure and large pore size.

## CHAPTER III EXPERIMENTAL

### 3.1 Materials

The chemicals which were used in this study, were listed in table 1

*Table 1: List of chemicals and source*

Chemical	Source
$\gamma$ -alumina ( $\gamma$ -Al <sub>2</sub> O <sub>3</sub> )	Galleon Brand
Silica (SiO <sub>2</sub> )	Fuji Davison
ZSM-5 zeolite (SiO <sub>2</sub> /Al <sub>2</sub> O <sub>3</sub> = 40)	TOSOH Company
Cobalt (II) nitrate hexahydrate [Co(NO <sub>3</sub> ) <sub>2</sub> .6H <sub>2</sub> O]	Alfa Aesa
Methanol (CH <sub>3</sub> OH, 99.8% purity)	RCI Labscan
Nitrogen (N <sub>2</sub> , 99.995% purity)	Praxair
Hydrogen (H <sub>2</sub> , 99.999% purity)	Praxair
Oxygen gas/Nitrogen gas (O <sub>2</sub> /N <sub>2</sub> = 1:99)	Praxair

### 3.2 Characterization of catalysts

The catalysts were characterized by nitrogen adsorption-desorption, X-ray diffraction (XRD), hydrogen temperature programmed reduction (H<sub>2</sub>-TPR), ammonia temperature programmed desorption (NH<sub>3</sub>-TPD) and thermogravimetric analysis (TGA).

#### 3.2.1. Nitrogen adsorption-desorption measurement

The surface area and pore size were measured in Quantachrom (AUTOSORB 1) at liquid nitrogen temperature (77K). The surface area was estimated by Brunauer-Emmett-Teller (BET) equation and total pore volume and pore size distribution were calculated by the Barrett-Joyner-Halenda (BJH) method.

### 3.2.2. X-ray diffraction (XRD)

X-ray diffraction (XRD) which was used to examine the bulk crystallinity of catalysts on Bruker D8 Advance equipped with  $\text{CuK}\alpha$  radiation at room temperature. The  $2\theta$  angle was scanned from 5 to  $80^\circ$  at the scan step of  $0.02^\circ$ . The Scherrer's equation applied at the most intense (311) diffraction ( $2\theta=36.9^\circ$ ) to estimate the  $\text{Co}_3\text{O}_4$  average particle size of calcined catalyst.

### 3.2.3. Temperature-programmed desorption of $\text{NH}_3$ ( $\text{NH}_3$ -TPD)

Temperature-programmed reduction ( $\text{H}_2$ -TPR) which was carried out in BELCAT (BEL JAPAN., INC) was used to study the acidity of catalyst. The sample was exposed to helium flow at  $500^\circ\text{C}$  for 1 hour. After cooling to  $100^\circ\text{C}$ , the sample absorbed 5% ammonia in helium (5% $\text{NH}_3/\text{He}$ ). The temperature of sample was increased at the rate of  $5^\circ\text{C}/\text{min}$  from  $100^\circ\text{C}$  to  $930^\circ\text{C}$ . Schematic of temperature program for TPD measurement are shown in Figure 2. The  $\text{NH}_3$  desorption was monitored in a thermal conductivity detector (TCD)

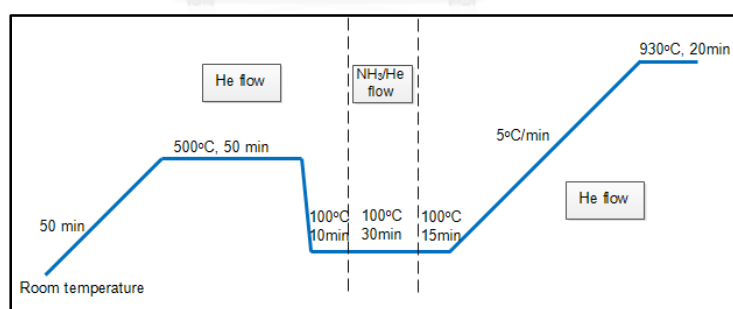


Figure 2: Schematic of temperature-program of TPD

### 3.2.4. Temperature-programmed reduction of $\text{H}_2$ ( $\text{H}_2$ -TPR)

Temperature-programmed reduction ( $\text{H}_2$ -TPR) which was carried out in BELCAT (BEL JAPAN., INC) was used to study the reduction behavior of metal oxidation state. The sample was pretreated at  $500^\circ\text{C}$  in argon to remove trace of water and cooled

down to 100°C. Then, the sample was exposed to reduce in 5% hydrogen in argon (5% $H_2$ /Ar) while the temperature was raised at the rate of 5°C/min from 100°C to 930°C. Schematic of temperature program of TPR measurement are exhibited in Figure 3. The consumption of  $H_2$  was monitored in a thermal conductivity detector (TCD).

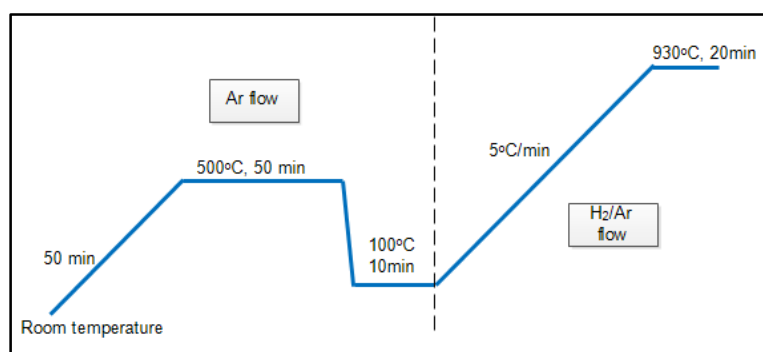


Figure 3: Schematic of temperature-program of TPR

### 3.2.5. Thermogravimetric analysis (TGA)

Thermogravimetric analysis were used to estimate coke on catalyst. It were carried out on TGA/DSC 1 (Mettler Toledo) instrument in oxygen flow of 20ml/min, with temperature range from 100 to 800°C at a linear ramping rate of 10°C/min.

### 3.3. Catalyst preparation

The impregnation method was chosen to prepare catalyst because of simplicity and rapidity.

The supports which were used in this study, include  $\gamma$ -alumina ( $\gamma$ - $Al_2O_3$ ), silica ( $SiO_2$ ) and ZSM-5 (H-MFI-40,  $SiO_2/Al_2O_3=40$  in molar ratio). They were dried in the oven at 120°C overnight. As for commercial ZSM-5, it was calcined in the furnace at 600°C for 3 hours

The cobalt-based catalysts containing 10 wt.% cobalt were prepared by incipient wetness impregnation method. The aqueous solution of cobalt nitrate obtains from cobalt (II) nitrate hexahydrate [ $Co(NO_3)_2 \cdot 6H_2O$ ] precursor impregnated on

supports. The catalysts after impregnation were dried at 120°C overnight, and finally calcined at 400°C for 5h in air to decompose nitrate ion.

The Co/ZSM-5 and ZSM-5 were sieved from 355 to 710µm particles before they were loaded into the reactor.

### 3.4. Catalyst reduction

The cobalt catalyst used in batch reactor and large scale fixed-bed reactor were reduced before charging into reactor. The reduction of catalysts was conducted in stainless steel tubular reactor. Before reduction, the catalyst was flushed in nitrogen at 120°C for 1h. The catalysts were reduced in H<sub>2</sub> flowing at 40 ml/min as temperature was ramped at 5°C/min to 400°C and then held for 10h. After reduction, the catalysts were cooled to room temperature and passivated in 1%O<sub>2</sub> in N<sub>2</sub> at flow rate 5ml/min for 10h before storage.

### 3.5. The catalytic apparatus

#### 3.5.1. Batch reactor

Catalyst performance was conducted in a 250ml batch reactor (Parr Instrument Co.,). The methanol of 63 g and catalyst at different loading were charged in the reactor. The following reaction conditions were investigated at 300°C under 1 bar initial pressure of N<sub>2</sub>. The schematic diagram of reactor is displayed in Figure 4. After the reaction, the reactor was cooled down to room. The gas and liquid products were collected and then, analyzed offline by Agilent gas chromatograph (GC 7890B) and gas chromatograph (Agilent GC 7820A) connected to mass spectrometry (Agilent MSD 5975).

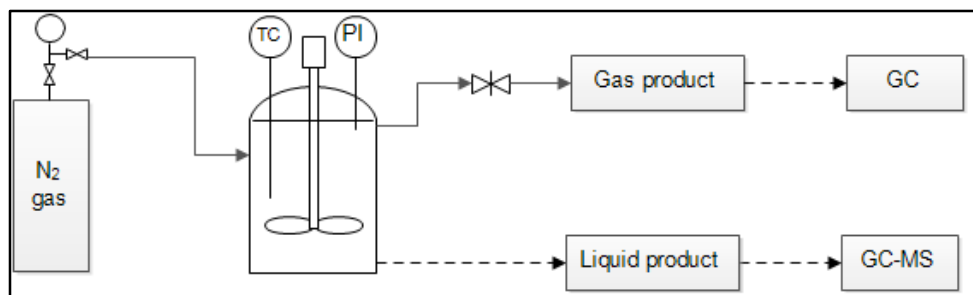


Figure 4: Schematic diagram of batch reactor

### 3.5.2. Fixed-bed reactor

#### 3.5.2.1. Larger scale

The effects of reaction conditions over  $\text{Co}/\gamma\text{-Al}_2\text{O}_3$  on methanol conversion and product selectivity were carried out in a fixed-bed reactor. The reactor was made of stainless steel with 20mm internal diameter. And, the reactor which was heated at middle part, was 450mm total length. The catalyst was charged 2.5g at the middle of reactor. Prior to apply the reaction condition, the catalyst was reduced in  $\text{H}_2$  flowing at 100 ml/min when the temperature was ramped at  $5^\circ\text{C}/\text{min}$  to  $400^\circ\text{C}$  and held at this temperature for 2h. After reduction, methanol conversion was investigated at following reaction condition: temperature  $300 - 450^\circ\text{C}$ , pressure atm to 10 bar, flow rate of methanol 0.1 to 0.5 ml/min. The reactor was purged with nitrogen before and after reaction. For every experiment, the feed was pumped by HLPC pump (Scientific Systems, Inc. Series II). Methanol was preheated at  $150^\circ\text{C}$ . This stream was mixed with nitrogen and passed through the reactor. The gas and liquid products were collected from the gas-liquid separator after cooling. The schematic diagram of large scale fixed-bed reactor is presented in Figure 5. The effluent gas were tested online by Agilent gas chromatograph (GC 7890B) while the liquid product were tested offline by gas chromatograph (Agilent GC 7820A) equipped with mass spectrometry (Agilent MSD 5975).



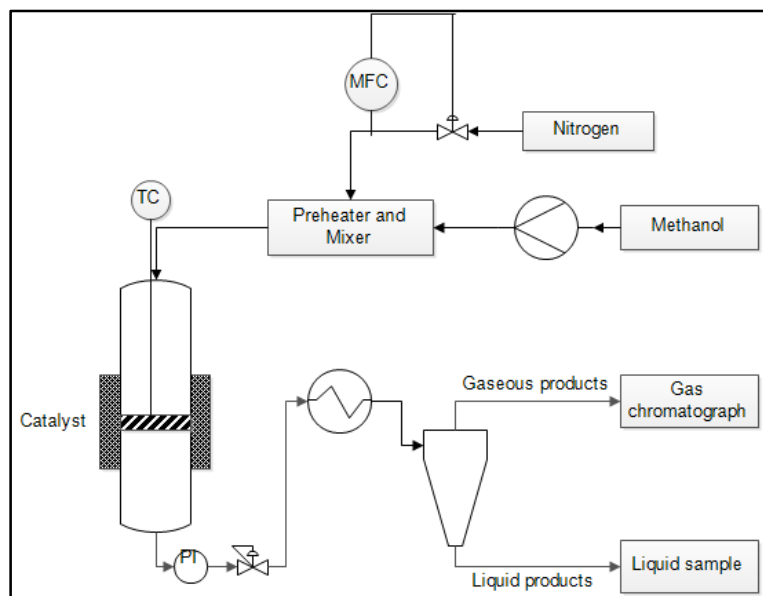


Figure 5: Schematic diagram of fixed-bed reactor

### 3.5.2.2. Small scale

The catalytic activity of cobalt-based catalyst and mixture of  $\text{Co}/\gamma\text{-Al}_2\text{O}_3$  and ZSM-5 catalyst were investigated in the fixed-bed reactor. Before the reaction, the cobalt catalyst was reduced in  $\text{H}_2$  flow of 20ml/min at  $400^\circ\text{C}$  for 2h. After reduction, the catalyst was cooled to the reaction temperature. Methanol was fed into reactor at flow rate of 0.1ml/min. The reaction condition was studied as follows: temperature  $300 - 400^\circ\text{C}$ , atmospheric pressure, flow rate of methanol 0.1ml/min. The schematic diagram small scale fixed-bed reactor is shown in Figure 6. The effluent gas was tested online by gas chromatograph (Shimadzu GC 14B). Liquid products were collected in an ice-bath cold trap and then were offline analyzed by gas chromatograph (GC 7820A) connected to mass spectrometry (5975MSD).

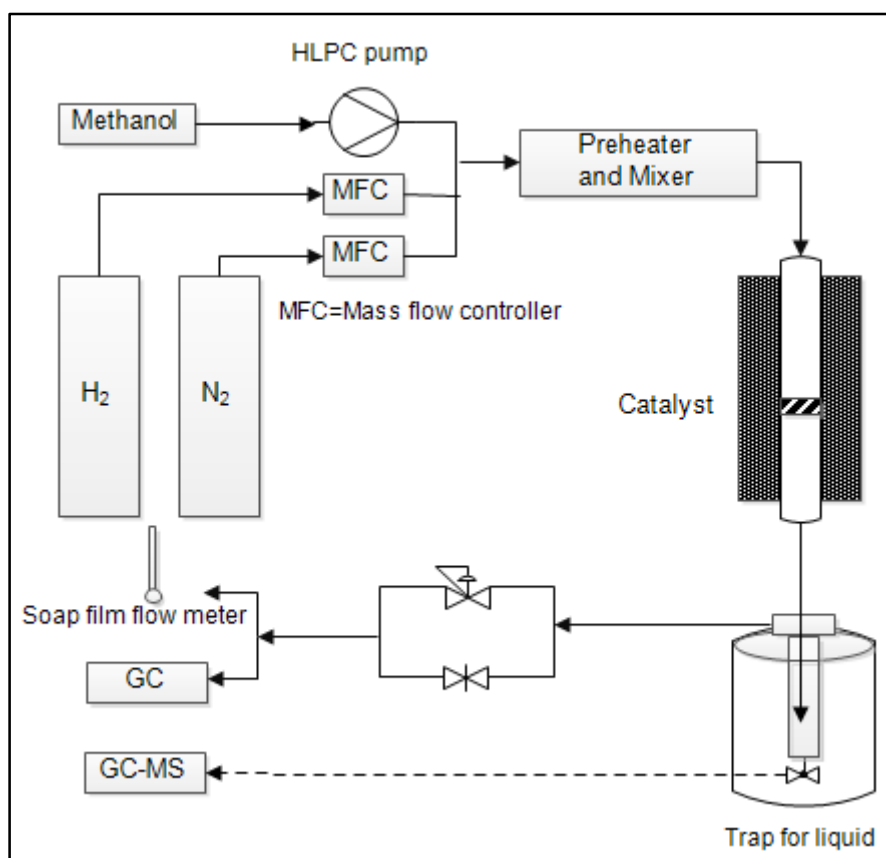


Figure 6: Schematic diagram of small scale fixed-bed reactor

### 3.5.2.3. Product analysis

The gas samples from batch reactor and large scale fixed-bed reactor were analyzed by using Agilent gas chromatograph (GC 7890B) equipped with two detectors including thermal conductivity detector (TCD) and flame ionization detector (FID). The TCD detector and MolSieve 13X were used for determination of CO, CO<sub>2</sub>, H<sub>2</sub> formed during reaction and carrier gas N<sub>2</sub> while the FID detector and Porapak Q-HT column were used for determination of hydrocarbons.

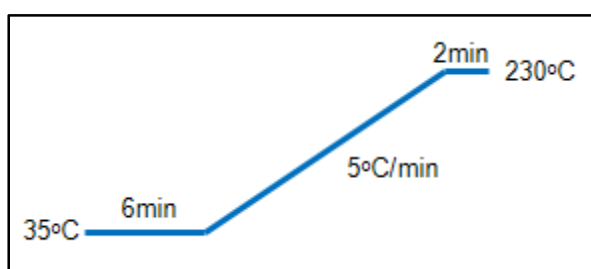


Figure 7: The GC heating program for gas analysis

The effluent gas from small scale fixed-bed reactor was detected online by gas chromatograph (Shimadzu GC 14B). While CO, CO<sub>2</sub>, H<sub>2</sub> and N<sub>2</sub> were analyzed by thermal conductivity detector (TCD) and Unibeads C column, the C<sub>1</sub> to C<sub>5</sub> light hydrocarbon gas were analyzed by flame ionization detector (FID) and Porapak Q column.

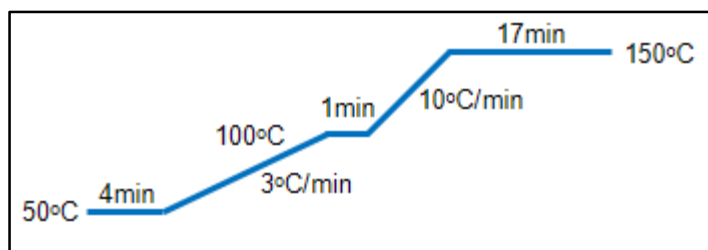


Figure 8: The GC heating program for gas analysis

The liquid products were identified and analyzed by using gas chromatograph-mass spectrometry (GC-MS) obtained from Agilent. The GC 7820A equipped with DB5-MS column (30m x 0.25mm x 0.25µm). The GC 7820A connected to mass spectrometry (Agilent 5975 MSD).

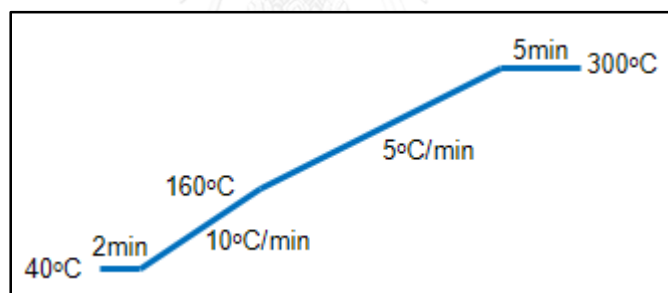


Figure 9: The GC-MS program for liquid analysis

## CHAPTER IV

### RESULTS AND DISCUSSION

#### 4.1. Characterization of catalysts

##### 4.1.1. Nitrogen adsorption-desorption

The loading of cobalt impacted on the surface of support. The textual properties, including BET surface area, average pore diameter, pore volume of support and cobalt-based catalyst as well as  $\text{Co}_3\text{O}_4$  crystallite size were compared in table 2

*Table 2: Textual properties and  $\text{Co}_3\text{O}_4$  crystallite size ( $d_{\text{Co}_3\text{O}_4}$ ) of support and catalyst*

Catalyst	BET surface area (m <sup>2</sup> /g)	Average pore diameter (nm)	Pore volume (cm <sup>3</sup> /g)	$d_{\text{Co}_3\text{O}_4}$ <sup>a</sup> (nm)
$\gamma$ -Al <sub>2</sub> O <sub>3</sub>	218.8	9.49	0.519	-
SiO <sub>2</sub>	306.9	18.37	1.409	-
ZSM-5	574.6	2.63	0.378	-
Co/ $\gamma$ -Al <sub>2</sub> O <sub>3</sub>	170.5	8.71	0.380	25.6
Co/SiO <sub>2</sub>	226.8	17.62	1.028	16.3
Co/ZSM-5	261.7	2.29	0.151	47.2

<sup>a</sup> The crystallite size of  $\text{Co}_3\text{O}_4$  was calculated by using Scherrer's equation (Appendix A.2).

From Table 2, it clears that the deposition of cobalt precursor on support reduced the surface area, average pore diameter and pore volume. It can be explained by the reason of partial blockage of pores by cobalt oxide cluster and partial collapse of mesoporous structure [28].

##### 4.1.2. X-ray diffraction

The XRD pattern of ZSM-5 and cobalt-based catalyst with different supports were shown in Figure 10.

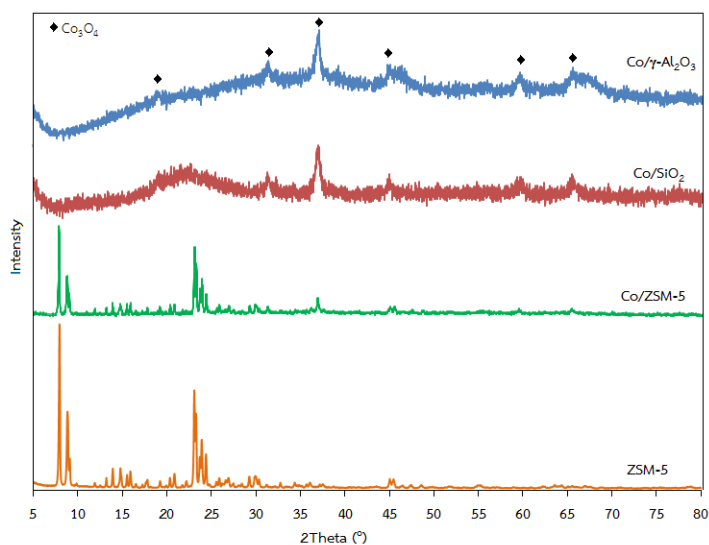


Figure 10: XRD patterns of ZSM-5, Co/ZSM-5, Co/SiO<sub>2</sub>, and Co/ $\gamma$ -Al<sub>2</sub>O<sub>3</sub> catalysts

According to XRD result of cobalt catalyst, the Co<sub>3</sub>O<sub>4</sub> pattern peaks were detected at  $2\theta = 18.9, 31.2, 36.7, 44.6, 59.3,$  and  $65.2$ . The group of detectable peaks agrees with recent report [27]. The difference in support did not affect to the intensities of these peaks. In addition, XRD analysis also confirmed the presence of MFI framework of ZSM-5 catalyst. The loading of Co make ZSM-5 crystallinity decrease.

The Co<sub>3</sub>O<sub>4</sub> crystallite size was calculated from Co<sub>3</sub>O<sub>4</sub> diffraction angle at  $2\theta = 36.7$ , then it was calculated by using Scherrer's equation as shown in table 2. As the result, the type and surface properties of support impact on the formation of Co<sub>3</sub>O<sub>4</sub>. The result shows that the size of Co<sub>3</sub>O<sub>4</sub> is larger than pore diameter of  $\gamma$ -Al<sub>2</sub>O<sub>3</sub> and ZSM-5. It can be explained that almost of the Co<sub>3</sub>O<sub>4</sub> spices disperse on the external surface of support due to small average pore diameter and pore volume. On the contrary, when Co was loaded on SiO<sub>2</sub>, the crystallite size of Co<sub>3</sub>O<sub>4</sub> is smaller than pore diameter of SiO<sub>2</sub>. It can be considered that the Co<sub>3</sub>O<sub>4</sub> spices can be deposited on the internal and external surface of SiO<sub>2</sub> because the average pore diameter and pore volume of SiO<sub>2</sub> are greater than that of  $\gamma$ -Al<sub>2</sub>O<sub>3</sub> and ZSM-5.

#### 4.1.3. Temperature-programmed desorption (NH<sub>3</sub>-TPD)

Temperature-programmed desorption of ammonia, which was used to evaluate the acidity of catalysts, is shown in Figure 11.

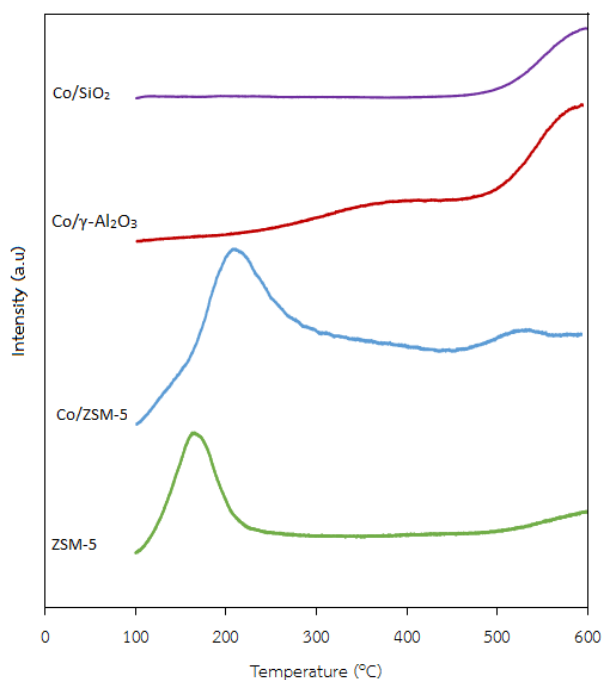


Figure 11:  $\text{NH}_3$ -TPD profiles of ZSM-5 and Co-based catalysts

The acidity of cobalt-based catalysts depends dramatically on the support. In comparison between ZSM-5 and Co/ZSM-5, the Co loading leads the weak acidic peak shift to higher temperature as well as acid sites to increase. Moreover, the strong acidic peak appears in Co/ZSM-5. The acid sites descend from Co/ZSM-5 to Co/ $\gamma$ - $\text{Al}_2\text{O}_3$ . The Co/ $\gamma$ - $\text{Al}_2\text{O}_3$  catalyst shows only medium acidic peak. On the contrary, Co/ $\text{SiO}_2$  catalyst performs none of acidity due to neutral acidic support of  $\text{SiO}_2$ .

#### 4.1.4. Temperature-programmed reduction ( $\text{H}_2$ -TPR)

To determine the reducibility of the  $\text{Co}_3\text{O}_4$  species, the three  $\text{H}_2$ -TPR patterns of Co-based catalysts are exhibited in Figure 12. All catalysts showed two main reduction peaks in temperature range of 200°C to 550°C. These peaks correspond to the reduction of  $\text{Co}_3\text{O}_4$  to  $\text{Co}^\circ$  with  $\text{CoO}$  as intermediate specie. However, the reducibility depends on the kind of supports. These peaks of Co/ $\gamma$ - $\text{Al}_2\text{O}_3$  are shifted to higher temperature when comparing with Co/ $\text{SiO}_2$  and Co/ZSM-5. It can be explained by the higher degree of interaction between metal and support. In addition, the Co/ZSM-5 and Co/ $\gamma$ - $\text{Al}_2\text{O}_3$  patterns provide some details. The first peak indicates the decomposition of cobalt nitrate remaining after calcination and the final peak can be

attributed the reduction of cobalt aluminate which is the strong interaction between Co and support.

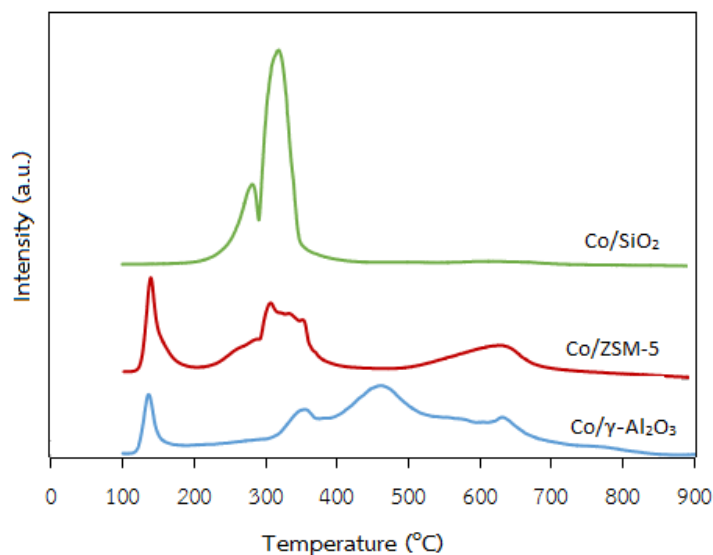


Figure 12:  $H_2$ -TPR pattern of Co-based catalysts

#### 4.2. The catalytic activity of cobalt-based catalyst

The effect of reaction parameters on methanol conversion and hydrocarbon distribution were investigated in batch and fixed-bed reactor. The main products of methanol conversion consist of light paraffins ( $C_2$ - $C_6$ ), light olefins ( $C_2$ - $C_5$ ) and heavy hydrocarbons ( $C_7$ - $C_{17}$ ). Moreover, the by-product such as  $CH_4$ , CO and  $CO_2$  is reported.

##### 4.2.1. Batch reactor

The batch reactor was used to study process parameter including reaction time and catalyst weight percent influencing to methanol conversion and product distribution

##### 4.2.1.1. Effect of reaction time

The effect of reaction time on conversion and product selectivity were shown in Table 3 and Figure 13.

Table 3: The effect of reaction time on methanol conversion and product distribution

mol.%	Time (h)		
	1	2	3
Conversion	18.85	76.61	45.25
Yield			
Methane	12.31	20.45	15.21
Light paraffin	2.73	4.59	3.57
Light olefin	0.25	0.31	0.14
C <sub>7</sub> <sup>+</sup>	0.27	3.27	0.04
Other	3.05	47.98	26.25

Reaction condition: 63g of methanol, 0.63g of Co/ $\gamma$ -Al<sub>2</sub>O<sub>3</sub>, 1 bar initial pressure of N<sub>2</sub>, 300°C

Reaction time affected significantly to methanol conversion. The increase in reaction time from 1 to 2 hours resulted in increasing methanol conversion, but it was dropped when the reaction time is longer. This phenomena can be explained that the forming of coke inside the pores of catalyst.

Reaction time also influenced to hydrocarbon distribution. The result showed that trace olefin can be detected in this system. The increase in reaction time slightly affected to light paraffin selectivity. Heavy hydrocarbon increased when applying reaction time from 1 to 2 hours, but it declined as a result of coke formation when the reaction time longer. This phenomena is displayed clearly in Figure 13. The amount of hydrocarbons, especially longer chain hydrocarbons were dramatically increased when reaction time extended from 1h to 2h but it dropped steeply when reation time was lasted for 3h.



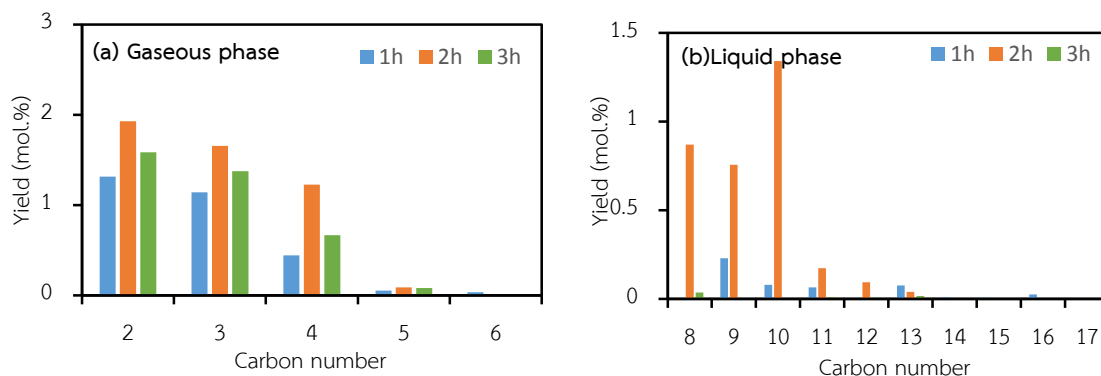


Figure 13: Effect of reaction time on product distribution in (a) gaseous phase and (b) liquid phase; reaction condition: 63g of methanol, 0.63g of  $\text{Co}/\gamma\text{-Al}_2\text{O}_3$ , 1 bar initial pressure of  $\text{N}_2$ ,  $300^\circ\text{C}$

#### 4.2.1.2. Effect of catalyst weight percent

The catalyst weight percent is the ratio of catalyst weight and reactant. The effect of catalyst weight percent on conversion and product selectivity were shown in Table 4 and Figure 14.

Table 4: Effect of catalyst weight percent on methanol conversion and product distribution

mol.%	Catalyst weight percent (%)		
	1	2	3
Conversion	76.61	84.63	86.12
Yield			
CH <sub>4</sub>	20.45	35.72	42.58
Light paraffin	4.59	8.20	10.35
Light olefin	0.31	0.13	0.04
C <sub>7</sub> <sup>+</sup>	3.27	2.11	1.34
Other	47.98	38.48	29.01

Reaction condition: 63g of methanol,  $\text{Co}/\gamma\text{-Al}_2\text{O}_3$ , 1 bar initial pressure of  $\text{N}_2$ ,  $300^\circ\text{C}$ , 2h reaction time.

The conversion increased with increasing amount of catalyst. The result showed that trace olefin was produced in this system. However, increasing in amount of

catalyst resulted to reduce heavy hydrocarbon selectivity slightly but extend the chain of hydrocarbon. It was clearly exhibited in Figure 14. The longer chain hydrocarbon dropped in batch reactor when 3% of catalyst was used. It can be explained that the production of longer chain hydrocarbon leads to form coke at higher catalyst loading. The result is explicit that the light paraffin were produced more when increasing in loading amount of catalyst. Moreover, the rise in methane selectivity suppressed the formation of other hydrocarbons.

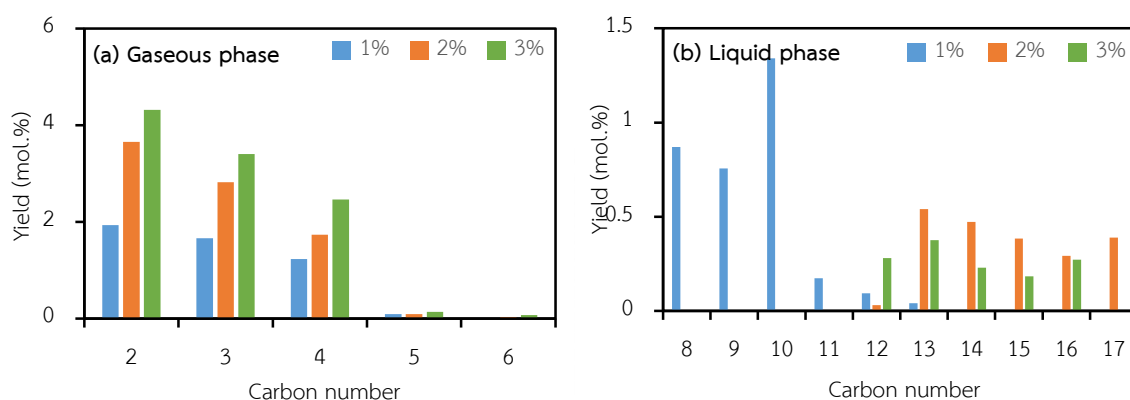


Figure 14: Effect of catalyst weight percent on product distribution in (a) gaseous phase and (b) liquid phase; reaction condition: 63g of methanol,  $\text{Co}/\gamma\text{-Al}_2\text{O}_3$ , 1 bar initial pressure of  $\text{N}_2$ ,  $300^\circ\text{C}$ , 2h reaction time.

In conclusion, reaction time and catalyst weight percent act on conversion of methanol to hydrocarbon. The longest chain hydrocarbon can be reached  $\text{C}_{17}$  with applying 2% of catalyst weight for 2h. However, the conversion and yield of total hydrocarbon product using 2% catalyst are less than that over catalyst loading of 3%.

#### 4.2.2. Large scale fixed-bed reactor

The reaction condition for methanol conversion were investigated over  $\text{Co}/\gamma\text{-Al}_2\text{O}_3$  in fixed-bed reactor.

##### 4.2.2.1. Effect of temperature

The effect of temperature on methanol conversion over  $\text{Co}/\gamma\text{-Al}_2\text{O}_3$  catalyst was shown in Table 5.

Table 5: Effect of temperature on methanol conversion and hydrocarbon distribution

mol.%	Temperature (°C)			
	300	350	400	450
Conversion	78.46	85.16	85.23	98.37
Yield				
CH <sub>4</sub>	2.06	4.68	8.13	8.40
Light paraffin	1.14	0.37	0.36	0.40
Light olefin	0.45	1.14	1.23	0.53
Other	74.81	78.96	75.52	89.05

Reaction condition: P= atm, F<sub>MeOH</sub>= 0.5 ml/min, 2.5g of Co/ $\gamma$ -Al<sub>2</sub>O<sub>3</sub>.

There is considerable influence of temperature on methanol conversion. The rise in temperature, the methanol conversion increased slightly from 300°C to 350°C, and unchanged from 350°C to 400°C. The conversion jumped up to nearly 100% when temperature reached 450°C. There is no heavy hydrocarbon produced in this system. The yield of paraffin reduced slowly while the methane formation increased sharply due to the rise in temperature from 300°C to 450°C. The rise in temperature affected to methanol conversion and the amount of methane formation were reported [6]. Light olefin products were raised gradually from 300°C to 400°C but declined suddenly from 400°C to 450°C. Moreover, the rise in temperature leads to decrease chain of hydrocarbon and increase by-products, especially 450°C. It can be explained that higher temperature favored cracking of methanol. The effect on hydrocarbon distribution was displayed in Figure 15.

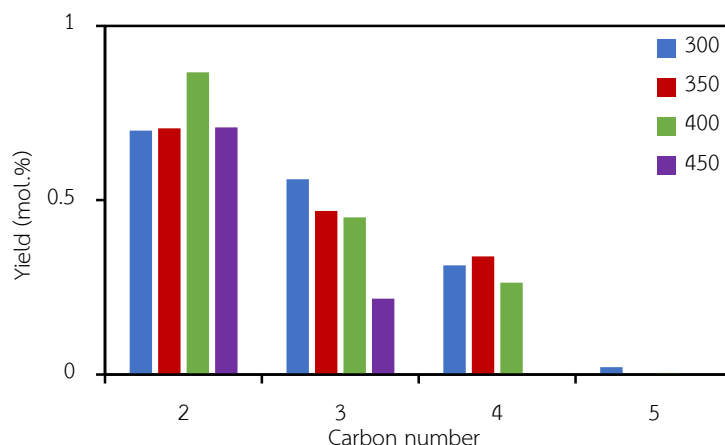


Figure 15: Effect of temperature on product distribution

( $P = \text{atm}$ ,  $F_{\text{MeOH}} = 0.5 \text{ ml/min}$ ,  $2.5 \text{ g of Co}/\gamma\text{-Al}_2\text{O}_3$ )

#### 4.2.2.2. Effect of pressure

The conversion of methanol to hydrocarbon was affected with the change in pressure. It was shown in Table 6 and Figure 16.

Table 6: Effect of pressure on methanol conversion and product distribution

mol.%	Pressure (bar)		
	1	5	10
Conversion	85.23	86.14	70.31
Yield			
CH <sub>4</sub>	8.13	32.80	43.26
Light paraffin	0.36	2.16	4.04
Light olefin	1.23	2.27	2.20
Other	75.52	48.92	20.81

Reaction condition:  $T = 400^\circ\text{C}$ ,  $F_{\text{MeOH}} = 0.5 \text{ ml/min}$ ,  $2.5 \text{ g of Co}/\gamma\text{-Al}_2\text{O}_3$

The increase in pressure from 1 to 5 bar unaffected to methanol conversion, but applying more pressure at 10 bar clearly influenced to drop in its conversion. Figure 16 presents the influence of pressure on product selectivity. There is no heavy hydrocarbon produced in this system. The acceleration of pressure leads to increase in main product and decrease in formation of by-products. The yield of paraffins, and olefins increased significantly while the pressure rose from 1 bar to 10 bar. In addition, the acceleration of pressure leads to extend the chain of hydrocarbon. It can be

explained that CO which was decomposed from methanol can be hydrogenated to hydrocarbon. The chain of hydrocarbon can be lengthened over Co-based catalyst when the higher pressure was applied.

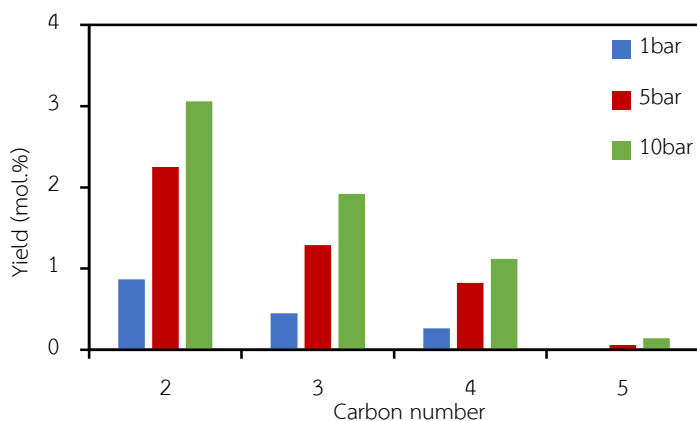


Figure 16: Effect of pressure on product distribution  
( $T=400^{\circ}\text{C}$ ,  $F_{\text{MeOH}} = 0.5\text{ml/min}$ , 2.5g of  $\text{Co}/\gamma\text{-Al}_2\text{O}_3$ )

#### 4.2.2.3. Effect of feed flow rate

The feed flow rate affected slightly on the conversion of methanol to hydrocarbon. The change in conversion of methanol was shown in Table 7 and Figure 17.

Table 7: Effect of feed flow rate on methanol conversion and product distribution

mol.%	Feed flow rate (ml/min)		
	0.1	0.25	0.5
Conversion	94.74	97.06	85.23
Yield			
CH <sub>4</sub>	11.58	8.59	8.13
Light paraffin	1.20	0.93	0.36
Light olefin	0.99	0.58	1.23
Other	80.97	86.96	75.52

Reaction condition:  $T=400^{\circ}\text{C}$ ,  $P=\text{atm}$ , 2.5g of  $\text{Co}/\gamma\text{-Al}_2\text{O}_3$

There was small decrease in methanol conversion when feed flow rate rise from 0.1 to 0.25ml/min, but conversion dropped at higher flow rate of feed. Light

paraffins fell slowly with the increase in feed flow rate while light olefin fluctuated. It can be considered that the lower flow rate of feed leads to extend the residence time that promotes the formation of hydrocarbon. However, the formation of by-products competes against hydrocarbon formation.

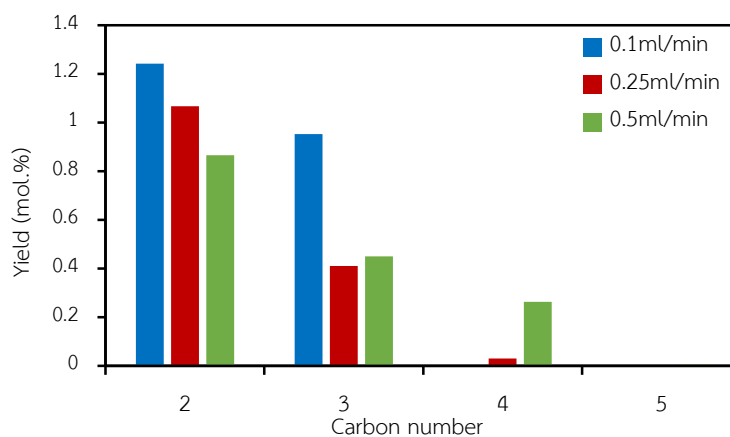


Figure 17: Effect of feed flow rate on product distribution  
( $T=400^{\circ}\text{C}$ ,  $P=\text{atm}$ ,  $2.5\text{g}$  of  $\text{Co}/\gamma\text{-Al}_2\text{O}_3$ ).

In summary, the methanol conversion and product distribution were significantly affected by reaction condition. The longer chain hydrocarbon can be achieved at low temperature and high pressure. Moreover, the increase in temperature and decrease in pressure provided that the conversion rose due to more by-products. Total yield of hydrocarbon was not be influenced by the change in temperature, excluding at  $450^{\circ}\text{C}$  but it stepped up with the rise in pressure. Conversely, when applying more feed flow rate, the conversion fluctuated but yield of total hydrocarbon dropped slightly.

#### 4.2.3. Small scale fixed-bed reactor

The catalytic activity cobalt-based catalyst and its combination with ZSM-5 were studied in small scale fixed-bed reactor.

##### 4.2.3.1. Effect of support

The effect of support on methanol conversion and hydrocarbon are shown in Table 8.

Table 8: Effect of support on methanol conversion and product distribution

mol.%	Catalyst		
	Co/ $\gamma$ -Al <sub>2</sub> O <sub>3</sub>	Co/SiO <sub>2</sub>	Co/ZSM-5
Conversion	96.42	95.06	86.64
Yield			
CH <sub>4</sub>	1.68	20.54	1.12
DME	21.91	1.09	16.87
Light paraffin	0.12	0.69	1.11
Light olefin	0.24	0.08	10.83
C <sub>7</sub> <sup>+</sup>			0.27
Other	72.47	72.65	56.43

Reaction condition: T=400°C, P=atm, F<sub>MeOH</sub>=0.1ml/min, 1g of catalyst

From Table 8, support types influenced slightly to methanol conversion but they affected significantly on product distribution. The conversion over Co/ $\gamma$ -Al<sub>2</sub>O<sub>3</sub> and Co/SiO<sub>2</sub> is nearly equal but it is higher than over Co/ZSM-5. The highest yield of total hydrocarbon was achieved over Co/ZSM-5. When using Co/ZSM-5 catalyst, light olefin is produced more than light paraffin. In addition, the longest chain hydrocarbon in gas phase can be formed over ZSM-5 support Co. It was shown clearly in Figure 18. The C<sub>7</sub><sup>+</sup> hydrocarbon can be detected in the liquid product when Co/ZSM-5 was used but it cannot be observed when  $\gamma$ -Al<sub>2</sub>O<sub>3</sub> and SiO<sub>2</sub> supported Co were used. It can be considered that the acid sites of Co/ZSM-5 is highest among three catalysts. Applying Co/ $\gamma$ -Al<sub>2</sub>O<sub>3</sub> yielded light paraffin and light olefin less than using Co/SiO<sub>2</sub>. DME production was obtained highest yield over Co/ $\gamma$ -Al<sub>2</sub>O<sub>3</sub> due to low acidity. The highest by-product were formed over Co/SiO<sub>2</sub>. It can be explained that the neutral acidity of Co/SiO<sub>2</sub> resulted in cracking reaction at 400°C.

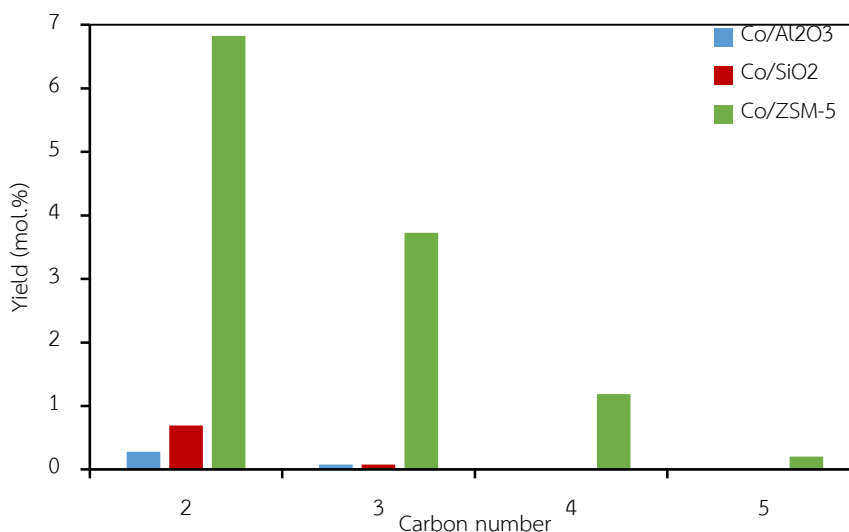


Figure 18: Effect of support on product distribution  
( $T=400^{\circ}\text{C}$ ,  $P=\text{atm}$ ,  $F_{\text{MeOH}}=0.1\text{ml/min}$ ,  $1\text{g}$  of catalyst)

#### 4.2.3.2. Effect of cobalt loading

The ZSM-5 catalyst has been utilized successfully for converting methanol to hydrocarbon. After loading cobalt on ZSM-5, the results are shown in negative effect on the conversion. However, DME and by-product were increased. The data are shown clearly in the Table 9.

Table 9: Effect of cobalt loading

mol.%	Catalyst	
	ZSM-5	Co/ZSM-5
Conversion	95.27	86.64
Yield		
CH <sub>4</sub>	4.84	1.12
DME	1.00	16.87
Light paraffin	27.96	1.11
Light olefin	32.22	10.83
C <sub>7</sub> <sup>+</sup>	23.08	0.27
Other	1.63	56.43

Reaction condition:  $T = 400^{\circ}\text{C}$ ,  $P=\text{atm}$ ,  $F_{\text{MeOH}} = 0.1\text{ml/min}$ ,  $1\text{g}$  of catalyst



In comparison with ZSM-5, the loading of cobalt leads to drop in yield of hydrocarbon as well as conversion while the yield of DME and by-product step up. It can be explained that the Co loading affect to reduce pore volume and surface area. Furthermore, Co active site promoted the cracking reaction at high temperature [29].

In summary, the cobalt-based catalysts were negative effect on the conversion methanol to hydrocarbons. However, the loading of cobalt is able to promote DME formation.

#### 4.2.3.3. Effect of separated or mixed beds of Co/ $\gamma$ -Al<sub>2</sub>O<sub>3</sub> and ZSM-5

The ZSM-5 and Co/ $\gamma$ -Al<sub>2</sub>O<sub>3</sub> were combined in different ways with ratio of 1:1. There were significant effect of separated and physical mixing catalysts on hydrocarbon distribution.

Table 10: Effect of separated or mixed beds of Co/ $\gamma$ -Al<sub>2</sub>O<sub>3</sub> and ZSM-5

mol.%	Catalyst			
	ZSM-5	ZSM-5 - Co/ $\gamma$ -Al <sub>2</sub> O <sub>3</sub> <sup>a</sup>	Co/ $\gamma$ -Al <sub>2</sub> O <sub>3</sub> - ZSM-5 <sup>b</sup>	ZSM-5 & Co/ $\gamma$ -Al <sub>2</sub> O <sub>3</sub> <sup>c</sup>
Conversion	95.27	88.36	97.62	96.50
Yield				
CH <sub>4</sub>	4.84	2.73	2.70	4.25
DME	1.00	21.42	0.03	0.00
Light paraffin	27.96	9.67	5.26	6.61
Light olefin	32.22	24.50	15.06	16.54
C <sub>7</sub> <sup>+</sup>	23.08	21.09	5.07	13.95
Other	1.63	6.38	69.07	52.85

Reaction condition: T = 400°C, P= atm, F<sub>MeOH</sub>= 0.1ml/min, 1g of catalyst, Co/ $\gamma$ -Al<sub>2</sub>O<sub>3</sub> : ZSM-5 = 1:1

<sup>a</sup> Separated beds of catalysts in order ZSM-5 and Co/ $\gamma$ -Al<sub>2</sub>O<sub>3</sub>.

<sup>b</sup> Separated beds of catalysts in order Co/ $\gamma$ -Al<sub>2</sub>O<sub>3</sub> and ZSM-5.

<sup>c</sup> Physical mixing of ZSM-5 & Co/ $\gamma$ -Al<sub>2</sub>O<sub>3</sub>.

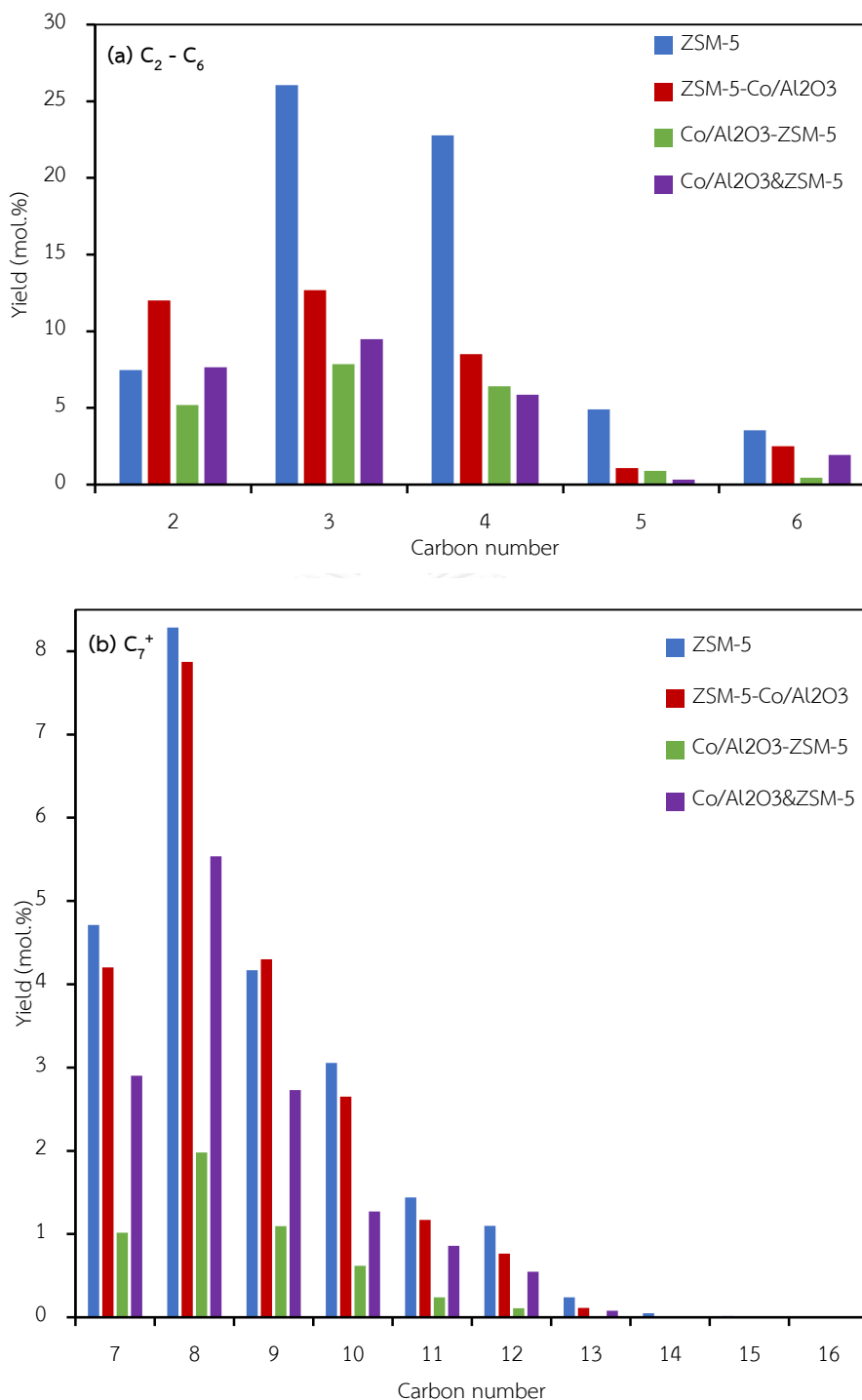


Figure 19: Effect of separated or mixed beds of Co/ $\gamma$ -Al<sub>2</sub>O<sub>3</sub> and ZSM-5 on product distribution in (a) C<sub>2</sub> - C<sub>6</sub> and (b) C<sub>7</sub><sup>+</sup> hydrocarbon product ( $T = 400^{\circ}\text{C}$ ,  $P = \text{atm}$ ,  $F_{\text{MeOH}} = 0.1\text{ml/min}$ ,  $1\text{g}$  of catalyst, Co/ $\gamma$ -Al<sub>2</sub>O<sub>3</sub> : ZSM-5 = 1:1)

From Table 10, the conversion were not change in all of the used catalysts. However, there are some different in yield of hydrocarbons. The highest yield of

hydrocarbons can be obtained over ZSM-5-Co/ $\gamma$ -Al<sub>2</sub>O<sub>3</sub>. Moreover, DME was achieved highest and by-product was formed lowest in comparison with other types, including Co/ $\gamma$ -Al<sub>2</sub>O<sub>3</sub>-ZSM-5 and ZSM-5 & Co/ $\gamma$ -Al<sub>2</sub>O<sub>3</sub>. It can be explained that the contact between methanol and first bed of ZSM-5 resulted in converting methanol to hydrocarbon, then remained methanol yielded DME over Co/ $\gamma$ -Al<sub>2</sub>O<sub>3</sub>. On the contrary, applying Co/ $\gamma$ -Al<sub>2</sub>O<sub>3</sub>-ZSM-5, the methanol converted over first bed of Co/ $\gamma$ -Al<sub>2</sub>O<sub>3</sub> to DME and by-products. After the remained methanol and DME reacted to produce hydrocarbon over second bed of ZSM-5. The highest by-products were formed over Co/ $\gamma$ -Al<sub>2</sub>O<sub>3</sub>-ZSM-5 due to cracking of methanol on Co/ $\gamma$ -Al<sub>2</sub>O<sub>3</sub>. When ZSM-5 & Co/ $\gamma$ -Al<sub>2</sub>O<sub>3</sub> was used, DME was synthesized over Co/ $\gamma$ -Al<sub>2</sub>O<sub>3</sub> while the mixture of methanol and DME converted to hydrocarbon. The trace of DME can be observed over Co/ $\gamma$ -Al<sub>2</sub>O<sub>3</sub>-ZSM-5 and ZSM-5 & Co/ $\gamma$ -Al<sub>2</sub>O<sub>3</sub> because it reacted with methanol to form hydrocarbon over ZSM-5.

From Figure 19, the yield of hydrocarbon is highest when ZSM-5 & Co/ $\gamma$ -Al<sub>2</sub>O<sub>3</sub> was used. The carbon number over ZSM-5-Co/ $\gamma$ -Al<sub>2</sub>O<sub>3</sub> were obtained until C<sub>14</sub>.

The hydrocarbon products can be reported in term of oil, gas (C<sub>2</sub>-C<sub>6</sub> and DME) and other (CH<sub>4</sub>, CO, and CO<sub>2</sub>). From Figure 20, the oil yield over ZSM-5 - Co/ $\gamma$ -Al<sub>2</sub>O<sub>3</sub> and ZSM-5 & Co/ $\gamma$ -Al<sub>2</sub>O<sub>3</sub> were obtained more than 5 wt.% which is higher than over Co/ $\gamma$ -Al<sub>2</sub>O<sub>3</sub>-ZSM-5.

At the same condition, three types of combined catalyst were compared with ZSM-5. Not only oil yield but also total hydrocarbon yield were higher than that over combined catalysts.

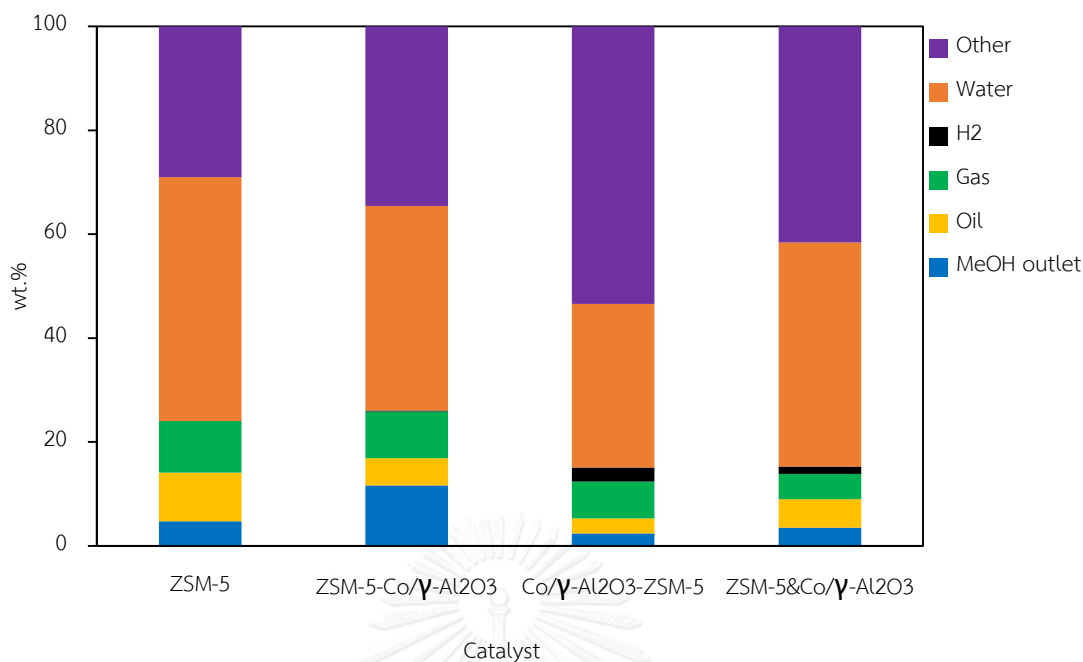


Figure 20: Effect of separated or mixed beds of  $\text{Co}/\gamma\text{-Al}_2\text{O}_3$  and ZSM-5 on product distribution in product weight percent ( $T = 400^\circ\text{C}$ ,  $P = \text{atm}$ ,  $F_{\text{MeOH}} = 0.1\text{ml}/\text{min}$ ,  $1\text{g}$  of catalyst,  $\text{Co}/\gamma\text{-Al}_2\text{O}_3 : \text{ZSM-5} = 1:1$ )

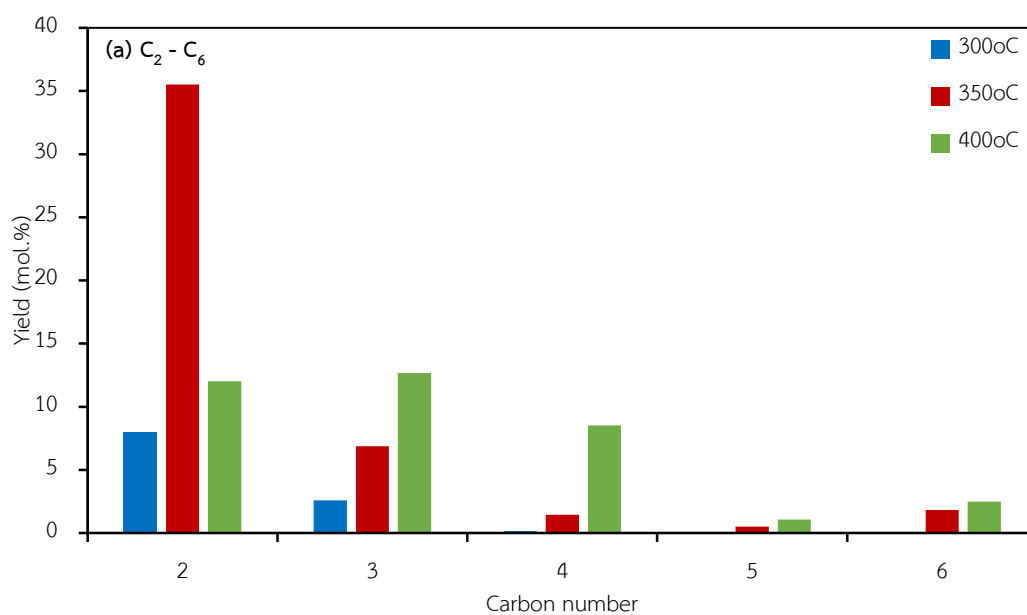
#### 4.2.3.4. Effect of temperature over separated beds of catalysts in order ZSM-5 and $\text{Co}/\gamma\text{-Al}_2\text{O}_3$ .

To investigate the effect of temperature over separated beds of catalysts in order ZSM-5 and  $\text{Co}/\gamma\text{-Al}_2\text{O}_3$  on conversion of methanol to hydrocarbon. From the data in Table 11, the conversion was not influenced by temperature range of  $300^\circ\text{C}$  to  $400^\circ\text{C}$ . However, temperature impacts greatly on yield of hydrocarbons as well as yield of oil. At  $300^\circ\text{C}$ , DME is the main product but the heavy hydrocarbon cannot be detected. In gaseous hydrocarbon, the light olefin is favored at  $350^\circ\text{C}$ , especially ethylene, but the composition of olefin hydrocarbon from  $\text{C}_3$  to  $\text{C}_6$  is lower than that at  $400^\circ\text{C}$ . The number of hydrocarbon can be obtained until  $\text{C}_{14}$  at  $400^\circ\text{C}$ . It is performed in Table 11 and Figure 21.

Table 11: Effect of temperature over separated beds of catalysts in order ZSM-5 and Co/ $\gamma$ -Al<sub>2</sub>O<sub>3</sub>.

mol.%	Temperature (°C)		
	300	350	400
Conversion	88.75	88.48	88.36
Yield			
CH <sub>4</sub>	0.35	2.03	2.73
DME	38.59	5.08	21.42
Light paraffin	1.14	3.38	9.67
Light olefin	9.64	40.36	24.50
C <sub>7</sub> <sup>+</sup>	0.00	22.69	21.09
Other	39.03	12.54	6.38

Reaction condition: P= atm, F<sub>MeOH</sub>= 0.1ml/min, ZSM-5 : Co/ $\gamma$ -Al<sub>2</sub>O<sub>3</sub> = 1:1, 1g of catalyst.



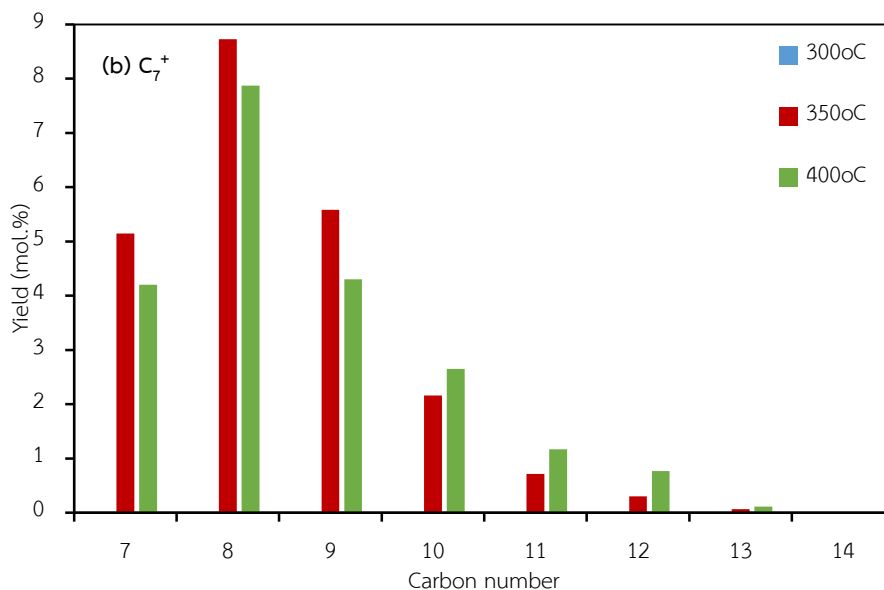


Figure 21: Effect of temperature on product distribution over separated beds of catalysts in order ZSM-5 and Co/ $\gamma$ -Al<sub>2</sub>O<sub>3</sub> in (a) C<sub>2</sub> – C<sub>6</sub> and (b) C<sub>7</sub><sup>+</sup> hydrocarbon product (P= atm, F<sub>MeOH</sub>= 0.1ml/min, ZSM-5 : Co/ $\gamma$ -Al<sub>2</sub>O<sub>3</sub> = 1:1, 1g of catalyst)

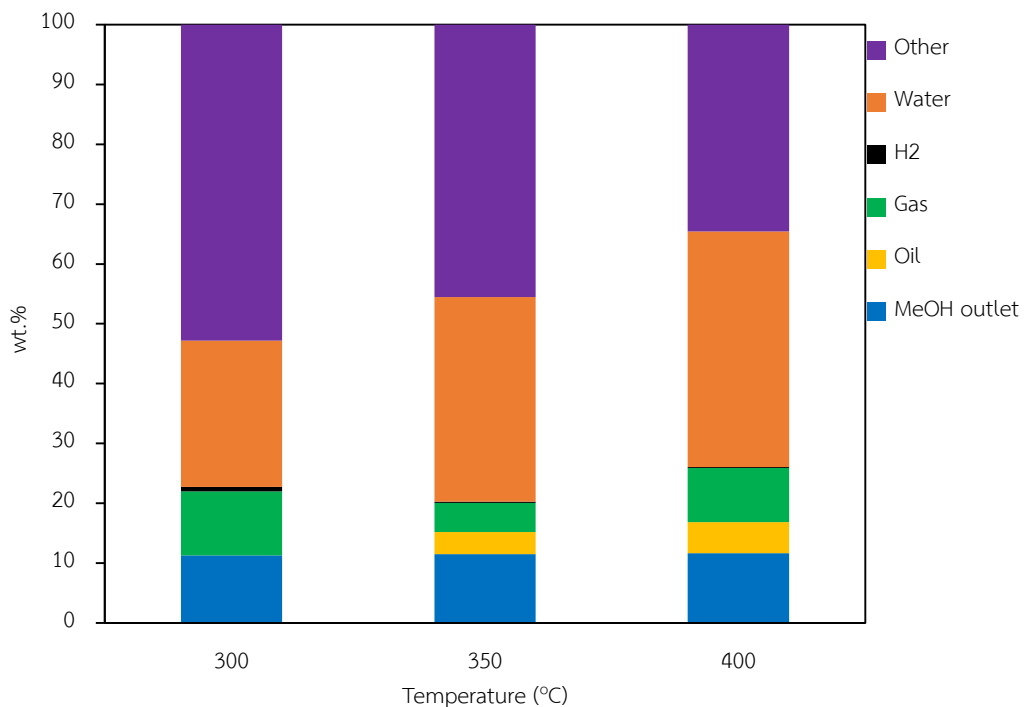


Figure 22: Effect of temperature on product distribution in product weight percent over separated beds of catalysts in order ZSM-5 and Co/ $\gamma$ -Al<sub>2</sub>O<sub>3</sub> (P= atm, F<sub>MeOH</sub>= 0.1ml/min, ZSM-5 : Co/ $\gamma$ -Al<sub>2</sub>O<sub>3</sub> = 1:1, 1g of catalyst)

The yield of oil climbed from 350°C to 400°C but it cannot be detected at 300°C due to the catalytic activity of ZSM-5. At 300°C, the combined catalysts favored the formation gaseous hydrocarbon, especially DME because DME is intermediate product which is favorable to be formed. It is shown in Figure 22.

In conclusion, the combination of ZSM-5 and Co/ $\gamma$ -Al<sub>2</sub>O<sub>3</sub>, the higher temperature is preferable to produce oil fraction in temperature range of 350-400°C.

#### 4.3. Stability of catalyst

The deactivation of catalyst was characterized by TGA and XRD technique. TGA was employed to evaluate the amount of carbon deposition. As the result shown in Figure 23, the weight loss of cobalt-based catalyst declined from 500°C and got unchanged at 650°C. It indicates the formation of coke on Co-based catalyst. Furthermore, the decrease in mass behaved differently. The highest coke can be observed on Co/SiO<sub>2</sub> due to the neutral acidity. The Co/SiO<sub>2</sub> favored to crack methanol at high temperature and then the deposition of carbon on surface deactivated catalyst. In comparison with Co-based catalyst, ZSM-5 catalyst performed none of coke formation.

From XRD pattern of spent catalyst, the Co<sub>3</sub>O<sub>4</sub> peak was disappeared due to transformation of Co<sub>3</sub>O<sub>4</sub> to Co<sup>0</sup> after reduction. The small peak which was detected at  $2\theta=45^\circ$ , can be attributed the Co<sup>0</sup> peak. It agrees with previous report [30]. After reaction, Co<sup>0</sup> did not be re-oxidated.

In summary, the cobalt-based catalyst can be deactivated by deposition of coke on the surface.

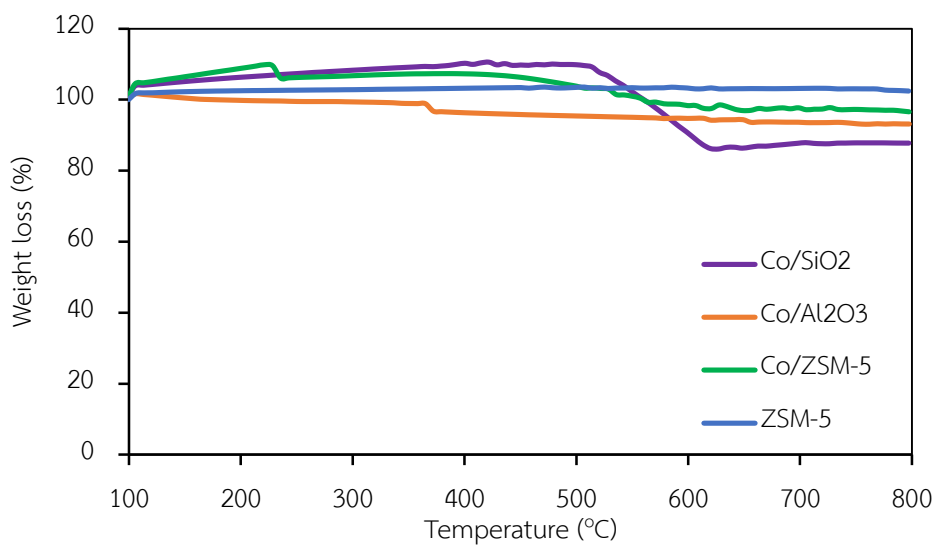


Figure 23: TGA profile of spent catalyst

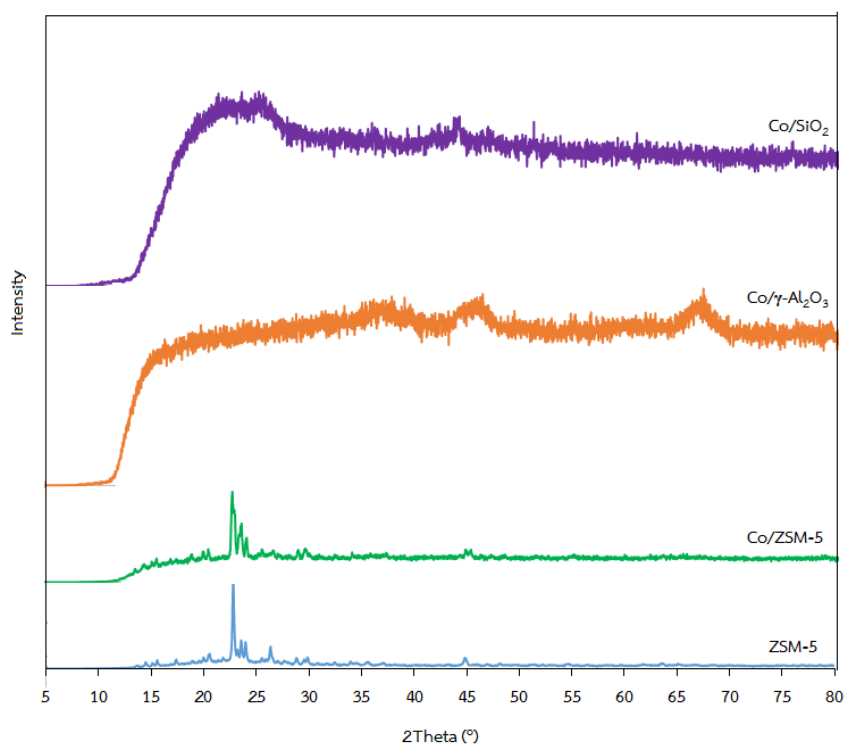


Figure 24: XRD pattern of spent catalysts



## CHAPTER V

### CONCLUSIONS AND RECOMMENDATIONS

#### 5.1 Conclusions

The effect of reaction condition on methanol to hydrocarbon over  $\text{Co}/\gamma\text{-Al}_2\text{O}_3$  was investigated in batch and fixed-bed reactor. In fixed bed reactor, the conversion raised while the paraffin selectivity reduced with the increase in temperature and decrease in pressure. In addition, the olefin yield rose when temperature and pressure increased but declined at higher temperature and pressure. However, heavy hydrocarbon cannot be detected in this system. On the contrary, olefin was produced as a trace in batch reactor. In batch reactor, the conversion and hydrocarbon yield reached maximum for 2 hours while the rise in catalyst weight percent leads to increase methanol conversion but the heavy hydrocarbon yield decrease. Nevertheless, paraffin selectivity is almost unaffected by reaction time but increased with the increase in catalyst amount.

The Co loading affected negatively on methanol to hydrocarbons due to formation short chain hydrocarbon, dimethyl ether as well as by-product. The support types influenced significantly on methanol conversion. The maximum hydrocarbon yield was achieved on  $\text{Co}/\text{ZSM-5}$ . The reason is that the higher selectivity to hydrocarbon was obtained at higher acidic support.

The various combination of  $\text{ZSM-5}$  and  $\text{Co}/\gamma\text{-Al}_2\text{O}_3$  was exhibited the dramatic change in hydrocarbons also yield of oil. The yield of oil over  $\text{ZSM-5-Co}/\gamma\text{-Al}_2\text{O}_3$  is as same as that over  $\text{ZSM-5}\&\text{Co}/\gamma\text{-Al}_2\text{O}_3$ . However,  $\text{ZSM-5-Co}/\gamma\text{-Al}_2\text{O}_3$  favored formation of hydrocarbon gas while  $\text{ZSM-5}\&\text{Co}/\gamma\text{-Al}_2\text{O}_3$  preferred to formation by-product. The methanol conversion to hydrocarbon over  $\text{ZSM-5-Co}/\gamma\text{-Al}_2\text{O}_3$  was obtained the highest yield of oil at  $400^\circ\text{C}$

The catalysts were deactivated by the formation of coke. However, the supports impact greatly on the amount of coke.

## 5.2 Recommendations

The ZSM-5 catalyst was used to convert methanol for hydrocarbon. However, the heavy hydrocarbon was obtained mainly from C<sub>7</sub> to C<sub>10</sub> due to the pore opening. The larger window opening of zeolitic support should be studied to lengthen the chain of hydrocarbon. Furthermore, the non-zeolitic support with acidity and large pore size improve the limitation of zeolite.

The loading of other metals, such as ion, chromium should be carried out because it could enhance the catalytic activity towards long chain hydrocarbon as well as the yield of oil fraction.



## REFERENCES

1. Olsbye, U., et al., *Conversion of methanol to hydrocarbons: how zeolite cavity and pore size controls product selectivity*. *Angewandte Chemie International Edition*, 2012. **51**(24): p. 5810-5831.
2. Olah, G.A., A. Goepfert, and G.S. Prakash, *Beyond oil and gas: the methanol economy*. 2006: John Wiley & Sons.
3. Chang, C.D. and A.J. Silvestri, *The conversion of methanol and other O-compounds to hydrocarbons over zeolite catalysts*. *Journal of Catalysis*, 1977. **47**(2): p. 249-259.
4. Lacarriere, A., et al., *Methanol to hydrocarbons over zeolites with MWW topology: Effect of zeolite texture and acidity*. *Applied Catalysis A: General*, 2011. **402**(1): p. 208-217.
5. Haw, J.F., et al., *The mechanism of methanol to hydrocarbon catalysis*. *Accounts of chemical research*, 2003. **36**(5): p. 317-326.
6. Zhao, W., et al., *Methane formation route in the conversion of methanol to hydrocarbons*. *Journal of Energy Chemistry*, 2014. **23**(2): p. 201-206.
7. Baerlocher, C., L.B. McCusker, and D.H. Olson, *Atlas of zeolite framework types*. 2007: Elsevier.
8. Stöcker, M., *Methanol-to-hydrocarbons: catalytic materials and their behavior*. *Microporous and Mesoporous Materials*, 1999. **29**(1): p. 3-48.
9. Chang, C.D., *Hydrocarbons from methanol*. *Catalysis Reviews Science and Engineering*, 1983. **25**(1): p. 1-118.
10. Flego, C., M. Marchionna, and C. Perego, *High quality diesel by olefin oligomerisation: new tailored catalysts*. *Studies in Surface Science and Catalysis*, 2005. **158**: p. 1271-1278.
11. Catani, R., et al., *Mesoporous catalysts for the synthesis of clean diesel fuels by oligomerisation of olefins*. *Catalysis today*, 2002. **75**(1): p. 125-131.

12. Lee, K.-Y., M.-Y. Kang, and S.-K. Ihm, *Deactivation by coke deposition on the HZSM-5 catalysts in the methanol-to-hydrocarbon conversion*. Journal of Physics and Chemistry of Solids, 2012. **73**(12): p. 1542-1545.
13. Iglesia, E., *Design, synthesis, and use of cobalt-based Fischer-Tropsch synthesis catalysts*. Applied Catalysis A: General, 1997. **161**(1): p. 59-78.
14. Khodakov, A.Y., et al., *Pore-size control of cobalt dispersion and reducibility in mesoporous silicas*. The Journal of Physical Chemistry B, 2001. **105**(40): p. 9805-9811.
15. Rane, S., et al., *Effect of alumina phases on hydrocarbon selectivity in Fischer-Tropsch synthesis*. Applied Catalysis A: General, 2010. **388**(1): p. 160-167.
16. Chu, W., et al., *Cobalt species in promoted cobalt alumina-supported Fischer-Tropsch catalysts*. Journal of Catalysis, 2007. **252**(2): p. 215-230.
17. De La Osa, A., et al., *Fischer-Tropsch diesel production over calcium-promoted Co/alumina catalyst: Effect of reaction conditions*. Fuel, 2011. **90**(5): p. 1935-1945.
18. Jun, K.-W., et al., *Highly water-enhanced H-ZSM-5 catalysts for dehydration of methanol to dimethyl ether*. BULLETIN-KOREAN CHEMICAL SOCIETY, 2003. **24**(1): p. 106-108.
19. Girardon, J.-S., et al., *Optimization of the pretreatment procedure in the design of cobalt silica supported Fischer-Tropsch catalysts*. Catalysis today, 2005. **106**(1): p. 161-165.
20. Pierella, L.B., et al., *Catalytic activity and magnetic properties of Co-ZSM-5 zeolites prepared by different methods*. Applied Catalysis A: General, 2008. **347**(1): p. 55-61.
21. Sartipi, S., et al., *Hierarchical H-ZSM-5-supported cobalt for the direct synthesis of gasoline-range hydrocarbons from syngas: Advantages, limitations, and mechanistic insight*. Journal of Catalysis, 2013. **305**: p. 179-190.
22. Tsakoumis, N.E., et al., *Deactivation of cobalt based Fischer-Tropsch catalysts: a review*. Catalysis Today, 2010. **154**(3): p. 162-182.

23. Park, J.W. and G. Seo, *IR study on methanol-to-olefin reaction over zeolites with different pore structures and acidities*. Applied Catalysis A: General, 2009. **356**(2): p. 180-188.
24. Hajimirzaee, S., et al., *Dehydration of methanol to light olefins upon zeolite/alumina catalysts: Effect of reaction conditions, catalyst support and zeolite modification*. Chemical Engineering Research and Design, 2015. **93**: p. 541-553.
25. Riad, M. and S. Mikhail, *Conversion of methanol to hydrocarbons on cobalt and lanthanum catalysts*. 2011.
26. ZENG, S.-h., et al., *Co/SBA-16: Highly selective Fischer-Tropsch synthesis catalyst towards diesel fraction*. Journal of Fuel Chemistry and Technology, 2014. **42**(4): p. 449-454.
27. Borg, Ø., et al., *Fischer-Tropsch synthesis over un-promoted and Re-promoted  $\gamma$ -Al<sub>2</sub>O<sub>3</sub> supported cobalt catalysts with different pore sizes*. Catalysis Today, 2009. **142**(1): p. 70-77.
28. Jung, J.-S., S.W. Kim, and D.J. Moon, *Fischer-Tropsch Synthesis over cobalt based catalyst supported on different mesoporous silica*. Catalysis Today, 2012. **185**(1): p. 168-174.
29. Meusinger, J., H. Vinek, and J. Lercher, *Cracking of n-hexane and n-butane over SAPO5, MgAPO5 and CoAPO5*. Journal of molecular catalysis, 1994. **87**(2): p. 263-273.
30. Grass, R.N. and W.J. Stark, *Gas phase synthesis of fcc-cobalt nanoparticles*. J. Mater. Chem., 2006. **16**(19): p. 1825-1830.

## APPENDIX

### A-1. Calculation for preparation of cobalt loading

Molecular weight of Co : MW = 58.93 g/mol

Molecular weight of  $\text{Co}(\text{NO}_3)_2 \cdot 6\text{H}_2\text{O}$  : MW = 291.31 g/mol

Catalyst 10wt% Co/ $\gamma\text{-Al}_2\text{O}_3$ , at weight of support = 10g

The amount of cobalt loading

$$m_{\text{Co}} = \frac{10 \times 10}{90} = 1.11g$$

The amount of cobalt nitrate required

$$m_{\text{Co}(\text{NO}_3)_2 \cdot 6\text{H}_2\text{O}} = \frac{1.11 \times 291.31}{58.93} = 5.49g$$

The pore volume of  $\gamma\text{-Al}_2\text{O}_3$ :  $V_p = 0.519 \text{ cm}^3/g$

The volume of water in cobalt nitrate

$$m_{\text{H}_2\text{O}} = \frac{5.49}{291.31} \times 6 \times 18 = 2.04g$$

The volume of water required with density  $d=1\text{g/ml}$

$$m_{\text{H}_2\text{O}} = 0.519 \times 10 \times 1 - 2.04 = 3.15g$$

## A-2. Calculation of crystalline size from X-ray Diffractometer (XRD)

The cobalt oxide ( $\text{Co}_3\text{O}_4$ ) particle can be estimated based on Scherrer equation

$$d(\text{Co}_3\text{O}_4) = \frac{\kappa\lambda}{\beta\cos\theta}$$

Where

$d(\text{Co}_3\text{O}_4)$  is the crystallite size of  $\text{Co}_3\text{O}_4$  (nm)

$\lambda$  is the X-ray wavelength ( $\text{CuK}\alpha = 0.154\text{nm}$ )

$\theta$  is the diffraction angel

$\kappa$  is a constant (usually  $\kappa = 1$ )

$\beta$  is the line broadening at half of the maximum intensity (in radian unit)

The cobalt particle size was calculated based on  $\text{Co}_3\text{O}_4$  particle size as equation following

$$D(\text{Co}^0) = 0.75d(\text{Co}_3\text{O}_4)$$

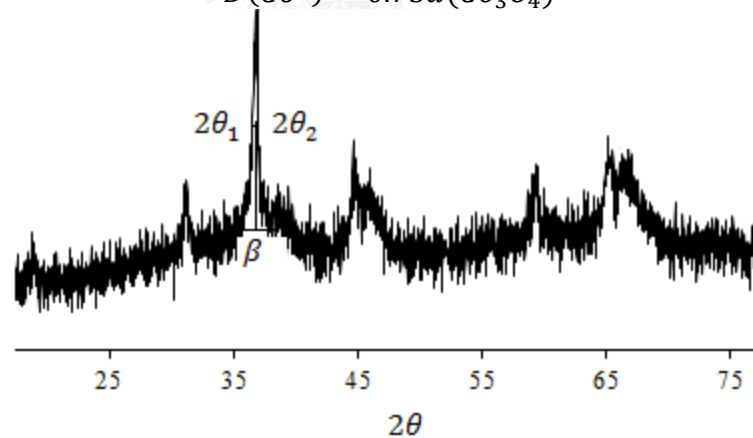


Figure 25: XRD pattern of  $\text{Co}/\gamma\text{-Al}_2\text{O}_3$

Example: 10wt%  $\text{Co}/\gamma\text{-Al}_2\text{O}_3$

$$2\theta_1 = 36.33^\circ, 2\theta_2 = 37.20^\circ, \theta = 0.87^\circ = \frac{\pi(0.87^\circ)}{180^\circ} = 0.015 \text{ radian}$$

$$\beta = \frac{\pi(0.365^\circ)}{180^\circ} = 0.006 \text{ radian}$$

$$d(\text{Co}_3\text{O}_4) = \frac{(1)(0.154)}{(0.006)\cos(0.015)} = 25.66\text{nm}$$

### A-3. Calculation for conversion of methanol in MTH reaction

The conversion of methanol to hydrocarbon was evaluated

$$\text{Methanol conversion (\%)} = \frac{(n_{in} - n_{out})}{n_{in}} \times 100$$

Where  $n_{in}$  = mole of methanol input

$n_{out}$  = mole of methanol output

### A-4. Calculation yield of hydrocarbon product

The yield of hydrocarbon product in gaseous and liquid phase was determined

$$\% \text{ Yield of hydrocarbon} = \frac{n_x}{n_{total}} \times \% \text{ conversion}$$

When  $n_x$  = carbon mole of interested component, mol

$n_{total}$  = carbon mole of total hydrocarbon, mol

### A-5. Calculation for weight percent of liquid and gaseous product

The weight percent of hydrocarbon was evaluated

$$\% \text{ Weight of oil product} = \frac{\text{wt. oil product}}{\text{wt. methanol}} \times 100$$

$$\% \text{ Weight of gas product} = \frac{\text{wt. gas product}}{\text{wt. methanol}} \times 100$$



## VITA

Miss Le Thi Ngoc Huyen was born on December 8, 1990 in Dong Thap province, Viet Nam. She graduated with Bachelor's degree of engineering, majoring in Petroleum and Petrochemical Technology, Faculty of Chemical Technology, Ho Chi Minh University of Industry, Ho Chi Minh city, Viet Nam in 2012. She has continued her study in Master program at Department of Chemical Technology, Faculty of Science, Chulalongkorn University since 2013 and finished her study in 2015.

### Presentation Experience

Poster presentation: Synthesis of hydrocarbons from methanol over cobalt/ $\gamma$ -alumina catalyst. Biotechnology International Congress (BIC) 2015 “Biotechnology for Healthy Society”, 9-10/9/2015, Bangkok, Thailand.

